





Supplementary Information for:

Development of targeted micelles and polymersomes prepared from degradable RAFT-based di-block copolymers and their potential role as nanocarriers for chemotherapeutics

Salma E. Ahmed, ^{abc} Nicholas L. Fletcher, ^{abc} Amber R. Prior, ^{abc} Pie Huda, ^{abc} Craig A. Bell, ^{*abc} and Kristofer J. Thurecht ^{*abc}

^a Australian Institute for Bioengineering and Nanotechnology, The University of Queensland, Brisbane, QLD, 4072, Australia. E-mail: k.thurecht@uq.edu.au.

^b Centre for Advanced Imaging, The University of Queensland, Brisbane, QLD, 4072, Australia.

^c ARC Centre of Excellence in Convergent Bio-Nano Science and Technology, The University of Queensland, Brisbane, QLD, 4072, Australia.

Contents

Characterisation methods	2
<i>In vitro</i> assays and confocal microscopy imaging	5
Synthesis of alkyne-functional xanthate CTA (3)	7
Synthesis of MeO-PEG macro-CTA	17
RAFT polymerisation of hydrophobic co-monomers using MeO-PEG macro-CTA	27
Cmc determination and self-assembly of the amphiphilic copolymers.....	34
<i>In vitro</i> cellular association and uptake studies.....	37
Minimum Information Reporting in Bio–Nano Experimental Literature.....	40
Checklist.....	40
Supplementary Table 1. Material characterization*	41
Supplementary Table 2. Biological characterization*	42
Supplementary Table 3. Experimental details*	43
References	44

Materials

α -Methoxy- ω -hydroxy poly(ethylene glycol) (MeO-PEG-OH, $M_n = 2000 \text{ g mol}^{-1}$, > 98%) was purchased from Iris Biotech GmbH, Germany. Cyanine-5- dibenzylcyclooctyne (Cy5-DBCO, $M_n = 929.03 \text{ g mol}^{-1}$, 95%) was purchased from Lumiprobe, USA. Dibenzylcyclooctyne-PEG₄-dibenzylcyclooctyne (DBCO-PEG₄-DBCO, $M_n = 854.92 \text{ g mol}^{-1}$, > 95%) was purchased from Click Chemistry Tools, USA. Ultrapure water with a resistivity of 18.2 M Ω .cm at 25 °C was obtained from an Elga ultra-pure water system. Vinyl acetate (VAc, >99%, Aldrich) was passed through an activated, basic alumina plug (Al₂O₃; Sigma-Aldrich, Brockmann I, standard grade, ~150 mesh, 58 Å pore size), to remove the inhibitor, and stored at -4 °C before use. Vinyl bromobutanoate (VBr) and 2-methylene-1,3-dioxepane (MDO) were synthesised as previously described by Hedir et al.[1] and Bailey et al.[2], respectively. 3-(4,5-dimethylthiazol-2-yl)-5-(3-carboxymethoxyphenyl)-2-(4-sulfophenyl)-2H-tetrazolium (MTS) assay (CellTiter 96 AQueous One Solution Cell Proliferation Assay; Promega) was used to assess cell viability.

Synthesis of xanthate precursors (1-3)

Firstly, carbon disulfide (250 mL, 4.16 mol, 34.5 mol eq.) was added to 4-methoxyphenol (15 g, 0.12 mol, 1 mol eq.) in a 1000 mL two-neck round bottom Schlenk flask, under inert conditions with continuous stirring at 40 °C. Upon complete dissolution of the reactants, triethylamine (Et₃N, 17 mL, 0.12 mol, 1 mol eq.) was added to the mixture, and the reaction was left to stir overnight. *Tert*-butyl 2-bromoacetate (11.4 mL, 0.12 mol, 1 mol eq.) was added dropwise under positive nitrogen pressure, and the reaction pot was left to stir at 40 °C for 2 days, after which a white precipitate formed at the bottom of the flask. Unreacted carbon disulfide was removed through vacuum transfer with a liquid nitrogen pre-trap, leaving a yellowish residue. This product was re-dissolved in 100 mL ethyl acetate, filtered, and followed by solvent extraction with distilled water (2 x 100 mL), sodium bicarbonate (sat.; 2 x 100 mL), *HCl* (1M; 2 x 100 mL), *distilled water* (2 x 100 mL), and brine (2 x 100 mL). The organic phase was collected, dried over anhydrous magnesium sulfate, filtered, and finally taken to dryness under a high vacuum. Column chromatography was performed using toluene as the mobile phase, then **1** was isolated and dried before collected as a pale-yellow oil (9.03 g, 24%).

Next, the BOC-group was removed by dissolving **1** (4 g, 12.7 mmol, 1 mol eq.) in dichloromethane (DCM, 80 mL) under inert conditions. After cooling to 0°C in an ice bath, *trifluoroacetic acid* (TFA, 12 mL, 12.23 mol eq.) was added dropwise and the reaction pot was left stirring overnight at room temperature. Excess DCM was evaporated using a rotary evaporator, while excess TFA was removed through vacuum transfer aided with a liquid nitrogen pre-trap. The product was recrystallised in toluene then collected by vacuum filtration to yield **2** as pale-yellow crystals (2.3 g, 71%).

To add alkyne functionality, **2** (0.5 g, 2 mmol, 1 mol eq.) was added to a round-bottom flask containing 4-dimethylaminopyridine (DMAP, 0.47 g, 4 mmol, 2 mol eq.) dissolved in 50 mL DCM. The reaction pot was left to cool in an ice bath under nitrogen before the addition of propargyl alcohol (0.22 g, 4 mmol, 2 mol eq.). *N*-ethyl-*n*'-carbodiimide hydrochloride (EDC.HCl, 0.93 g, 4.8 mmol, 2.5 mol eq.) was then added to the round-bottom flask and the reaction was left stirring overnight at room temperature. The organic solution was extracted with water (2 x 100 mL) and brine (2 x 100 mL) before being dried over anhydrous sodium sulfate. The solution was then filtered and reduced in volume to dryness. Column chromatography (silica) was conducted using DCM and methanol (9:1) as the mobile phase. After isolation and drying, **3** was collected as a pale-yellow powder (0.48 g, 71%).

Synthesis of PEG precursors and MeO-PEG macroCTA (4-6)

MeO-PEG-OH (5 g, 2.5 mmol, 1 mol eq.) was dissolved in 10 mL of dry DCM in an ice bath at inert environment, before the addition of methanesulfonyl chloride (MsCl, 1.4 g, 1 mmol, 5 mol eq.) under positive nitrogen pressure (moisture-sensitive reaction). Et₃N (1.74 mL, 12.5 mmol, 5 mol eq.) was added and the reaction was left to stir overnight. The organic solution was extracted with hydrochloric acid (6M, 2 x 100 mL), distilled water (2 x 100 mL), and brine (2 x 100 mL), then dried over anhydrous magnesium sulfate, filtered, and reduced in volume. The solution was precipitated into cold diethyl ether and collected by filtration to yield **4** as a white powder (4.7 g, 99%).

4 (4 g, 2 mmol, 1 mol eq.) was dissolved in 15 mL DMF (anhydrous), before the addition of sodium azide (1.59 g, 24.4 mmol, 12.5 mol eq.). The reaction pot was heated to 50 °C and left to stir overnight. The product was cooled to room temperature. DCM (35 mL) was then added, and the combined solution was extracted with cold distilled water (2 x 100 mL) and washed with cold brine (2 x 100 mL). The organic phase was dried over anhydrous magnesium sulfate, filtered, and reduced in volume. The solution was then precipitated into cold diethyl ether, filtered and dried *in vacuo*, and **5** was collected as a white powder (3.3 g, 81%).

Finally, **3** (59.3 mg, 0.2 mmol, 1 mol eq.) and **5** (0.5 g, 0.1 mmol, 0.5 mol eq.) were added to a Schlenk flask along with DMF (anhydrous, 3 mL) to make the MeO-PEG MacroCTA. To this solution was added *N,N,N',N'',N''*-pentamethyldiethylenetriamine (PMDETA, 3.5 μ L, 0.02 mmol, 0.1 mol eq.) before degassed with N₂ sparging for 15 min. Copper (I) bromide (CuBr, 2.9 mg, 0.02 mmol, 0.1 mol eq.) was then introduced under positive nitrogen pressure. After 2

hours of continuous stirring, excess CuBr was removed by passage through a short basic Al₂O₃ plug using DCM as the eluent. The organic phase was extracted with water (2 x 100 mL), dried over anhydrous magnesium sulfate, filtered, and reduced in volume. The concentrated polymer solution was precipitated into cold diethyl ether, filtered and dried *in vacuo*, and **6** was collected as a pale-yellow powder (352.8 mg, 77%).

RAFT terpolymerisation of VAc, MDO and VBr (7)

An example reaction for RAFT terpolymerisation of VAc, MDO and VBr is as follows:

For DP 200 (**7A**), 1,1'-azobis(cyclohexanecarbonitrile) (ABCN, 0.346 mg, 1.42 μmol, 0.1 mol eq.), **6** (32.5 mg, 14.2 μmol, 1 mol eq.), VAc (170.9 mg, 2 mmol, 140 eq.), MDO (64.7 mg, 0.567 mmol, 40 mol eq.) and VBr (54.7 mg, 0.28 mmol, 20 mol eq.) were dissolved in deuterated benzene (715.8 μL, 66 wt%) and transferred to a Young's tapped Schlenk ampoule, before degassing via three freeze-pump-thaw cycles. The ampoule was backfilled with argon, sealed, then heated to 90°C, and left to stir for 36 hours, before quenching at 0 °C. A small aliquot was reserved to determine monomer conversion using ¹H NMR spectroscopy. The remaining solution was diluted with CHCl₃ and precipitated into cold n-hexane (100 mL). The residue was redissolved in CHCl₃, and the precipitation process was repeated twice more. The resulting polymer was dried *in vacuo* prior to use.

Azidation and Cy5 labelling of the amphiphilic blocks (8 and 9)

As an example reaction for diblock copolymer azidation, **7A** (171 mg, 11.25 μmol) was dissolved in DMF (855 μL, 200 mg/mL), then sodium azide was added in excess (124 mg, 1.9 mmol, 10 mol eq. to VBr). The reaction was left to stir at room temperature for 2 days to allow it to reach full completion (i.e., 100% conversion). The product was then dissolved in DCM, and the organic phase was washed with brine (2 x 50 mL), dried over anhydrous magnesium sulfate, filtered, and reduced in volume *in vacuo*. The concentrated solution was precipitated into cold n-hexane, collected by centrifugation, then dried *in vacuo* at room temperature to afford **8A** as a waxy pale-yellow solid.

The hypothesis that the reaction conversion reached 100% was confirmed using proton NMR (Figure 4, part (i) to (ii)), where peak (i) has completely shifted upfield (from 3.45 ppm to 3.3 ppm), confirming hence the complete substitution of VBr to VN₃. The residual peak that remains in Figure 4, part (ii) is the spinning side band of the main PEG chain, as it is also evident and symmetrical on the other side of the PEG peak. Additionally, when taking the integration of peak (c) at 4.5 ppm as a reference (I_c=2), the values of the integration of peak (i+a) at 3.34 ppm were found to be identical in both, part (i) and part (ii) of Figure 4 (I_{i+a} = 31.91).

As an example reaction of the labelling process, **8A** (20.9 mg, 1.375 μmol, 1/17 mol VN₃ eq.) was dissolved in DMF (105 μL, 200 mg/mL) then Cy5-DBCO (2.2 mg, 2.337 μmol, 0.1 mol VN₃ eq.) was added. After 3 hours with continuous stirring at room temperature, the solution was dialysed for 4 hours to remove excess dye before precipitation into n-hexane (2 x 50 mL). The residue was collected by centrifugation and dried *in vacuo* to afford **9A** as a blue waxy solid.

Cy5-DBCO conjugation to the hydrophobic blocks was confirmed using 2D DOSY NMR, where all chains of 9A and 9B diffused as one band, as shown in the insets of Figure S26-(i) and (ii). The exact amounts of Cy5 attached in each polymer chain were calculated using UV-Vis, as shown in Figure 4-(iv). Furthermore, taking into consideration that all self-assembled NPs were dialysed (using 10K MWCO dialysis tubing) against excess amount of water (>1L water), and that the water has been changed at least once during the dialysis step, without detecting any blue colour in the dialysis water, we confirmed with confidence that the fluorescence signal of Cy5 when studying intracellular distribution of NPs, originated from the covalent-bonding with the hydrophobic blocks within the NPs.

Micelle and polymersome self-assembly

An example of self-assembly process to form micelles is as follows: 5 mg of **9A** was dissolved in DMF at a concentration of 5 mg/mL and stirred overnight to fully solvate the polymer. For the drug-loaded micelles, DOX.HCl (0.5 mg) was incorporated at a 10:1 polymer:drug ratio, along with Et₃N (0.12 μL, 1 mol DOX.HCl eq.) to neutralize the HCl. For the drug-loaded polymersomes, DOX.HCl (0.5 mg) was added at a 10:1 polymer:drug ratio, to be encapsulated within the vesicular hydrophilic core. PBS or water (9 mL) was then slowly introduced via a syringe pump at a flow rate of 0.6 mL/hr. The formed micellar suspension was either dialysis-purified (using ThermoFisher SnakeSkin™ dialysis tubing, 10K MWCO) to form non-crosslinked micelles, or incubated for an hour with 2 mg of DBCO-PEG₄-DBCO crosslinker (25 μL of a 50 mg/mL DMF stock solution) before dialysis to produce crosslinked micelles. 200 μL aliquots were lyophilised from each batch, before and after dialysis, to estimate drug loading capacity (LC%) and encapsulation efficiency (EE%).

Characterisation methods

¹H and ¹³C Nuclear Magnetic Resonance (NMR) spectra were recorded at 500 MHz on a Bruker Avance 500 high-resolution NMR spectrometer at 298 K. 1D and 2D proton diffusion spectra (DOSY) were recorded by increasing the

gradient strength (gpz6) linearly from 2 to 95% in 32 steps at ambient temperature (gradient length (δ)= 3000 μ s, diffusion time (Δ) = 100 ms). MestReNova software (v14.1) was used to process all NMR spectra.

ElectroSpray Ionization Mass Spectroscopy (ESI-MS) was measured by Waters Quattro Micro API ElectroSpray Ionization (ESI) Mass Spectrometry. Data was collected using 3 kV capillary voltage, 40 V cone voltage, 3 V extractor voltage, 0.2 V RF Lens voltage, source temperature of 120 °C, desolvation temperature of 150 °C, desolvation gas flowrate of 400 L/h, pump flow rate of 10 μ L/min, and mass filter MS1 scanning from m/z 50 to 650. Samples were prepared by filtering 0.1 mg/mL solutions in methanol through a 0.22 μ m PTFE microfilter.

High-Resolution Mass Spectrometry (HRMS) measurements were obtained using a Bruker Micro TOF Q II - ESI-Qq-TOF system, calibrated against an ESI calibration solution (ESI tune mix, Agilent G1969-8500). Samples were prepared by filtering 0.1 mg/mL solutions in methanol through a 0.22 μ m PTFE microfilter, and then aliquots were further diluted with purified methanol to obtain a final concentration of 5 μ g/mL.

Matrix-Assisted Laser Desorption/Ionization-Time of Flight (MALDI-ToF) mass spectroscopy analysis was conducted on a Bruker Daltonics Autoflex Speed MALDI-TOF/TOF mass spectrometer, used in a positive ion TOF detection mode and acceleration voltage of 25 kV, to obtain MS spectra of PEG-derivatives and macroCTA. Samples of 1 mg/ mL in Tetrahydrofuran (THF) were prepared, then 1 μ L aliquots were taken from each sample, mixed with equivalent volumes of α -cyano-4-hydroxycinnamic acid (α -CHCA, 30 mg/mL THF) matrix and sodium trifluoroacetate (NaTFA, 2 mg/mL in THF) ionisation agent, and finally spotted on an MTP 384 ground steel target plate and allowed to air dry. All measurements were conducted in the reflector ion mode and calibrated with a mixture of 2 and 5 kDa MeO-PEG-OH standards.

Size Exclusion Chromatography (SEC) was performed on a Waters SEC 1515 system, fitted with a 1515 isocratic pump, 717 auto-sampler, Styragel HT 6E and Styragel HT 3 columns, 2414 differential refractive index detector. Polystyrene standards (1.35 kDa to 1.3 MDa) were used for calibration, and fit to a third-order polynomial. All SEC samples were prepared by filtering 10 mg/mL solutions in THF through a 0.22 μ m PTFE microfilter before measuring their molecular weights and dispersities. THF was used as an eluent at a flow rate of 1 mL/min.

Fourier-transform infrared spectroscopy (FT-IR) spectra were measured by Agilent Cary 630 ATR-FTIR, fitted with a diamond crystal (Diamond ATR accessory), performing 32 background and sample scans. Transmission/absorption data produced was in the range of 4000 to 400 cm^{-1} .

Particle size and size distributions were measured by Dynamic Light Scattering (DLS) using a Zetasizer Nano ZS (Malvern Instruments) at 25 °C, using a backscatter angle of 173°. Samples were passed through a 0.45 μ m syringe filter before each measurement, equilibrated for 120 s before analysis, and then analysed in triplicate, where each replicate was measured 10 times to determine the average NP size. Polydispersity indices (PDI) were used to determine the particle size distribution and particle size uniformity.

Further confirmation of size and population distribution were provided using Transmission Electron Microscopy (TEM). Images were acquired using a Hitachi 7777 transmission electron microscope, operating at an acceleration voltage of 100 kV. 10 μ L of diluted samples were deposited onto 200-mesh carbon-coated copper grids that have been glow-discharged to increase their hydrophilicity. The samples were left for 3 min to air-dry before staining with 10 μ L of uranyl acetate (aq., 2%, w/v) for 2 min. Excess stain was removed with filter paper and TEM grids were left to dry under ambient conditions before use.

Ultraviolet-visible (UV-Vis) absorbance measurements were performed on either a Nanodrop 2000C spectrophotometer (Thermo Scientific) with a 10 mm path length using a quartz cuvette, or a Tecan Plate reader using a 96-well plate. Absorbance maxima were recorded at 490 and 642 nm for DOX (molar extinction coefficient $\epsilon = 10,410 \text{ cm}^{-1}\text{M}^{-1}$) and Cy5 ($\epsilon = 250,000 \text{ cm}^{-1}\text{M}^{-1}$), respectively. Fluorophore to polymer ratio in **9A** and **9B** were calculated using M_n and absorbance data (A , ϵ , l) from UV-Vis spectra after dissolving each polymer in THF at [10 mg/mL].

Critical micelle concentration (cmc) determination: The cmc was determined by observing the fluorescence signal omitted from free and encapsulated N-phenyl-1-naphthylamine (PNA) dye at the desired DP.¹ Briefly, a known volume of PNA stock solution (12 μ L; 4.56 mM, dissolved in ethanol) was mixed with 1 mL of the amphiphilic copolymers that were pre-prepared at different known concentrations. The mixtures were left stirring overnight at room temperature in a shaking incubator. The samples were passed through polycarbonate membranes with 0.45 μ m pore size to eliminate the excess dye before being aliquoted in a 96-well plate. PNA fluorescence signal was measured using a plate reader, at an excitation wavelength of 340 nm and emission wavelength range of 370-500 nm. Relative micellar intensity ($I_{\text{micelle}}/I_{\text{water}}$) was calculated as the maximum fluorescence intensity of aliquots at each concentration divided by the maximum fluorescence intensity of water (blank sample). These values were

normalised and plotted against the logarithmic values of the corresponding polymers concentrations. The intercepts between low and high concentration regions correspond to the cmc value of each polymer.

Stability Analysis of NP: 1500 μL of Roswell Park Memorial Institute (RPMI) 1640 (ThermoFisher Scientific) cell culture media (containing 50% FBS) was added to 500 μL of 0.6 mg mL^{-1} NP in PBS. The mixture was incubated at 37 °C for 15 days, where aliquots were taken at specific time intervals to test the sizes using DLS, then returned to the incubation vial. TEM imaging was also conducted to confirm the NP morphology, following 4 days of incubation (96 hours).

Encapsulation efficiency (EE %) and loading capacity (LC %): the DOX concentration in each batch was determined by observing UV-Vis absorbance at 490 nm and comparing the values against a previously established DOX-calibration curve. Drug LC% was calculated as (weight of loaded DOX / weight of loaded NP) \times 100%. EE % was calculated as (weight of loaded DOX / weight of DOX in feed) \times 100%.

***In vitro* assays and confocal microscopy imaging**

Cy5 was chosen as the imaging probe over other organic fluorophores as it is known for its high stability and robustness in optical visualisation.² Once the NP are self-assembled, Cy5 will be located either in the membrane of the polymersomes or the cores of the micelles. This design aspect offers the advantage of avoiding any alteration of the NP cellular uptake mechanism due to the additional hydrophobicity introduced via the conjugated fluorophores.³

***In vitro* release studies in buffered solutions:** A typical dialysis technique was used to establish *in vitro* release profiles for the formed DOX-loaded, crosslinked or non-crosslinked NP at pH values simulating the physiological and endosomal pH conditions (pH 7.4 and 5.2, respectively).⁴ Briefly, 1 mL of NP suspension (0.5 mg /mL) were dialysed in triplicates at 37 °C for 10 days against 25 mL of either phosphate- or citrate- buffered solutions (1X, pH 7.4 and 1X, pH 5.2, respectively). At specific time points, 200 μL aliquots were taken from the release media, and equivalent amounts of fresh buffers were added simultaneously, throughout the length of the release experiments (10 days). A plate reader was used to record the absorbance wavelength of DOX in each aliquot that diffused into the release media through the 3.5 kDa MWCO dialysis cassette. The readings were recorded against a previously established DOX calibration curve. The release experiments were conducted in triplicate, and the average percentage cumulative drug release was reported for each formulation.

Cell lines: EGFR-overexpressing and CD8 negative MDA-MB-468 breast cancer cell lines (ATCC HTB-132) were used to evaluate the cellular association and uptake of the NP. As per the American Type Culture Collection (ATCC, Manassas, VA, USA) guidelines, the cells were cultured in Gibco Dulbecco's Modified Eagle Medium (DMEM, Invitrogen), supplemented with 10% (v/v) fetal bovine serum (FBS, heat-inactivated, ThermoFisher Scientific), 100 mg mL^{-1} penicillin and 100 mg mL^{-1} streptomycin, and incubated at 37 °C in a humidified atmosphere of 5% CO_2 in air. All cells used in the *in vitro* cellular assays have passage number <20.

Introduction of targeting proteins: A humanised BsAb with binding affinity to EGFR and methoxy PEG was used to produce actively targeted NPs, namely, anti-human EGFR-anti-PEG NPs ($\alpha\text{EGFR-}\alpha\text{PEG-NPs}$).⁵ Non-targeted NPs were used as a control group, whereas NPs conjugated with another BsAbs that don't bind EGFR receptors, namely anti-PEG-anti-PEG ($\alpha\text{PEG-}\alpha\text{PEG}$) or anti-CD8-anti-PEG ($\alpha\text{CD8-}\alpha\text{PEG}$) were used as a negative controls.⁵ In all protein-decorated NPs, simple mixing of the former with the PEGylated NPs for 45 min at (0.01:1) BsAb/polymer chain molar ratio was sufficient to form strong non-covalent interactions to produce stable targeted NPs. In previous studies, this non-covalent bond is sufficiently stable in complex biological systems.⁶

Cellular association: To determine the degree of cellular association of the targeted (with EGFR-BsAb), non-targeted and negative controls, MDA-MB-468 cells were seeded in 1.5 mL Eppendorf tubes at a concentration of 1×10^5 cells/tube, before adding the treatments (i.e., control NP, negative control NP, targeted NP, or media only). The Eppendorf tubes were incubated in a humidified atmosphere of 5% CO_2 for 4 hours at 37 °C, after which they were centrifuged at 1400 rpm for 5 min and washed twice with phosphate-buffered saline (PBS) containing 5% FBS before suspending the treated cells in PBS/FBS. To further confirm the specific targetability of the targeted NP to the upregulated cellular EGFR, a simple flow cytometry blocking assay was followed. Briefly, an $\alpha\text{-EGFR}$ single-chain fragment variable ($\alpha\text{-EGFR scFv}$) at a concentration of 240 $\mu\text{g/mL}$ (e.g., (30:1) BsAb/polymer chain molar ratio) was incubated with 1×10^5 cells for 15 min to block the majority of the EGFR binding sites. Targeted NPs were then added and incubated with the cells in a humidified atmosphere of 5% CO_2 for one hour at 37 °C. The treated cells were then centrifuged at 1400 rpm for 5 min and washed twice with phosphate-buffered saline (PBS) containing 5% FBS before suspending them in PBS/FBS and keeping them in ice until tested. In both the cellular association and

blocking assays, data were acquired for 10,000 events/sample on a Cytoflex S (Beckman Coulter) flow cytometer. Forward and side scattering intensities were recorded. APC channel (660/10 nm) was used to record Cy5 main fluorescence intensities (MFI), and PE channel (585/42 nm) was used to record DOX MFI as well. FlowJo software (v 10.7.1) was used for gating and data analysis.

Confocal Laser Scanning Microscopy (CLSM): CLSM of treated cells was performed using a Zeiss 710 laser-scanning confocal microscope housed within the Australian National Fabrication Facility - Queensland Node (ANFF-Q). MDA-MB-468 cells were seeded in 35 mm MatTek glass bottom dishes at a density of 1×10^5 cells/ dish overnight, then treated with crosslinked, DOX-loaded (DOX concentration in each NP is $10 \mu\text{g mL}^{-1}$), targeted or non-targeted micelles or polymersomes, before being incubated in a humidified atmosphere of 5% CO_2 at 37 °C, for 5 hours (in live-cells experiments) or 12-hours (in fixed cells experiments). Similar to flow cytometry analysis, the dishes were washed gently with PBS to remove unbound NP. Cell fixation could be performed at this stage using paraformaldehyde (PFA) solution (4% in PBS buffer, 0.2 mL) applied for 10 minutes. Cellular nuclei were then stained with Hoechst 33342 fluorescent dye (Invitrogen; 10 mg/ mL, diluted 1:5000 in PBS) for 10 min before the final wash with PBS. A 40x water immersion lens was used to visualise the cells. Hoechst 33342, DOX and Cy5 fluorescence signals were collected in separate channels, excited with 350, 488 and 633 nm lasers, respectively. The data was collected using a sequential scanning method, between (460 – 490 nm), (500 – 700 nm) and (643 – 700 nm) for each track, respectively. The collected images were analysed on Zen software (v 3.3, blue edition), where linear unmixing followed by a Gaussian filter were applied on all images before data analysis to reduce binning artifacts, minimise spectral overlap, and produce smoother pixelated datapoints.

Cell viability assays: MTS assays were used to determine cell viabilities and toxicity profiles of the NPs. Briefly, MDA-MB-468 cancer cells were seeded into 96 well plates at a density of 1×10^4 cells per well. The cells were incubated overnight at 37 °C in 100 μL of complete DMEM growth media (containing 10% FBS). Following the incubation period, the media was discarded and replaced with equivalent volumes of fresh media, containing either free DOX, nascent NPs or DOX-loaded NPs (with or without EGFR-targeting). Seven DOX concentrations were used across the range 0.01-50 $\mu\text{g/mL}$, with each experiment conducted in triplicate. After incubating for two days, MTS was applied following the manufacturer's specifications to assess cell viability.

Statistical analysis: For sizing measurements and cytotoxicity studies, the data are presented as the average \pm SD ($n=3$). Statistical analysis of relative fluorescence intensity of DOX and Cy5 within the cells and nuclei obtained using CLSM, along with IC_{50} (half maximal inhibitory concentration required to produce 50% cell death) and cell cytotoxicity values were calculated using GraphPad Prism 7, and statistical differences between different groups were analysed using 2-way ANOVA, where ns > 0.05, *p-value < 0.05, **p-value < 0.005, ***p-value < 0.0005, and ****p-value < 0.0001.

Synthesis of alkyne-functional xanthate CTA (3)

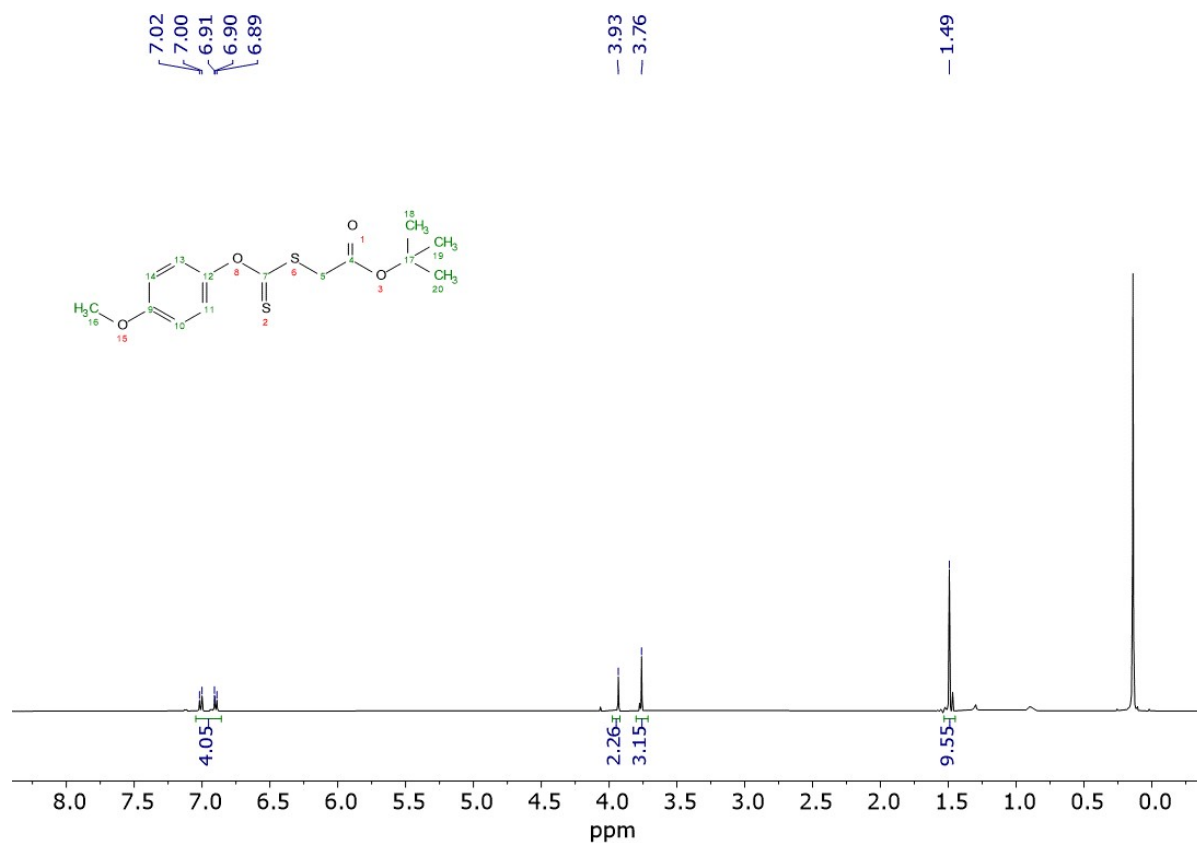


Figure S1. ¹H NMR (500 MHz, CDCl₃) spectrum of **1**.

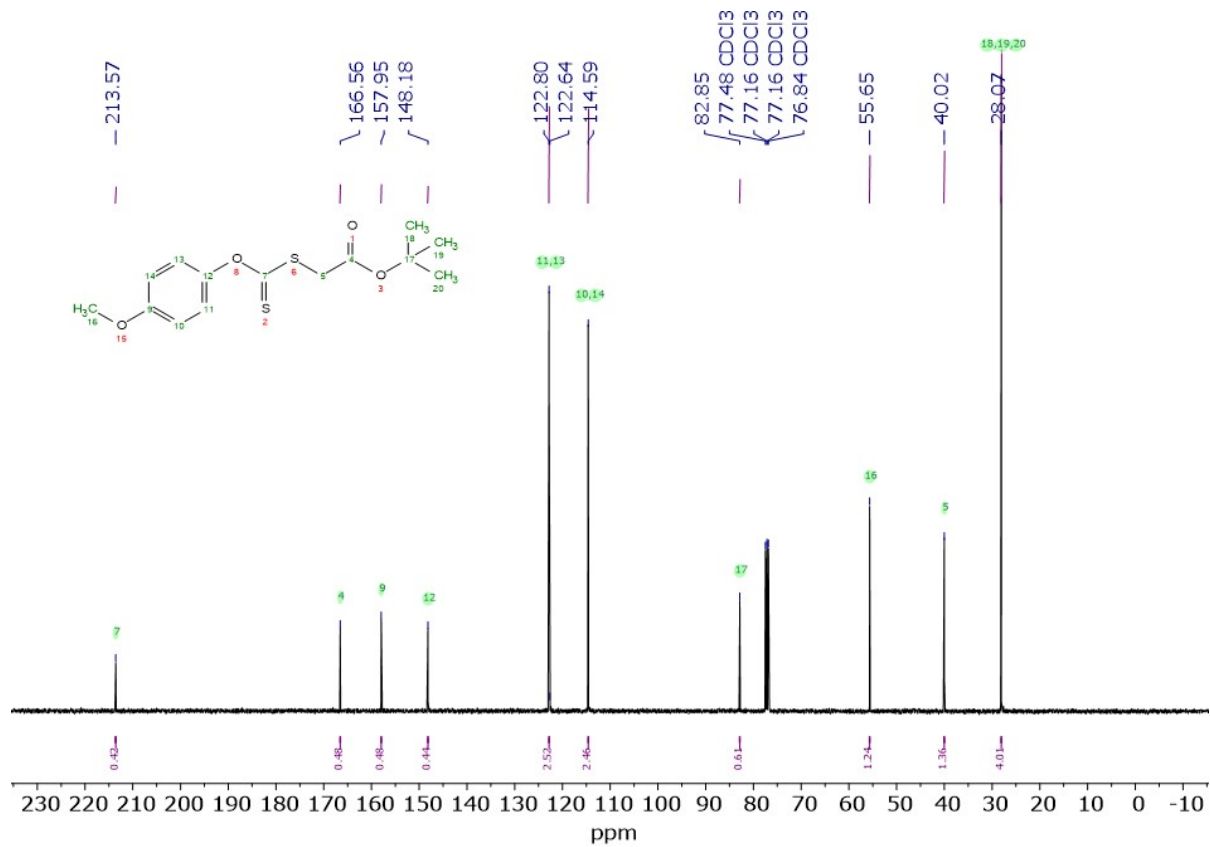


Figure S2. ^{13}C NMR (125 MHz, CDCl_3) spectrum of 1.

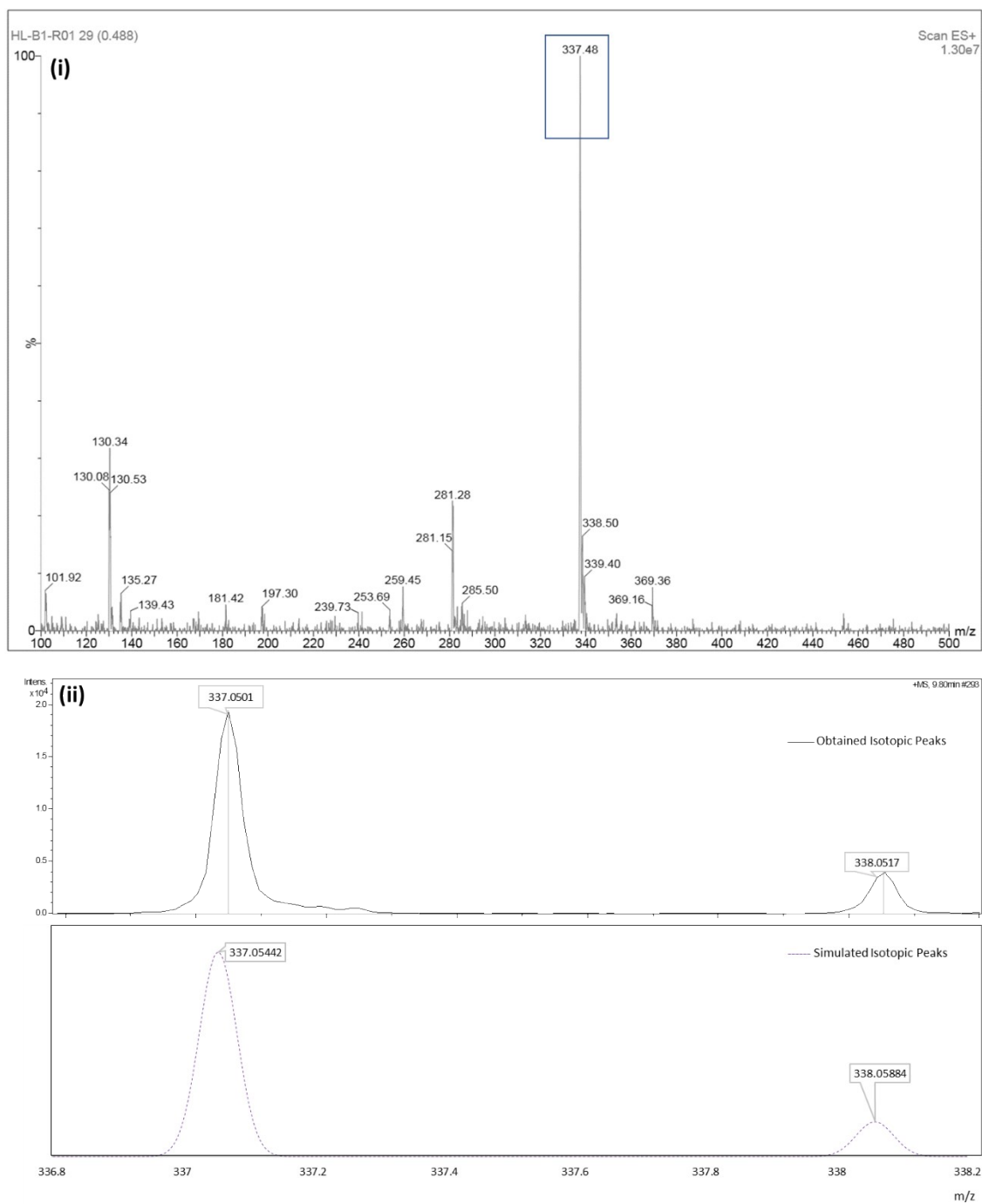


Figure S3. Mass spectroscopy of **1**. (i) ESI-MS spectrum, where 100 % abundant species is the $[M+Na]^+$ adduct. (ii) HRMS $[M+Na]^+$ of **1**, with the obtained isotopic peaks (top trace) versus the simulated isotopic peaks (bottom) for $C_{14}H_{18}O_4S_2Na^+ = 337.0544$ m/z.

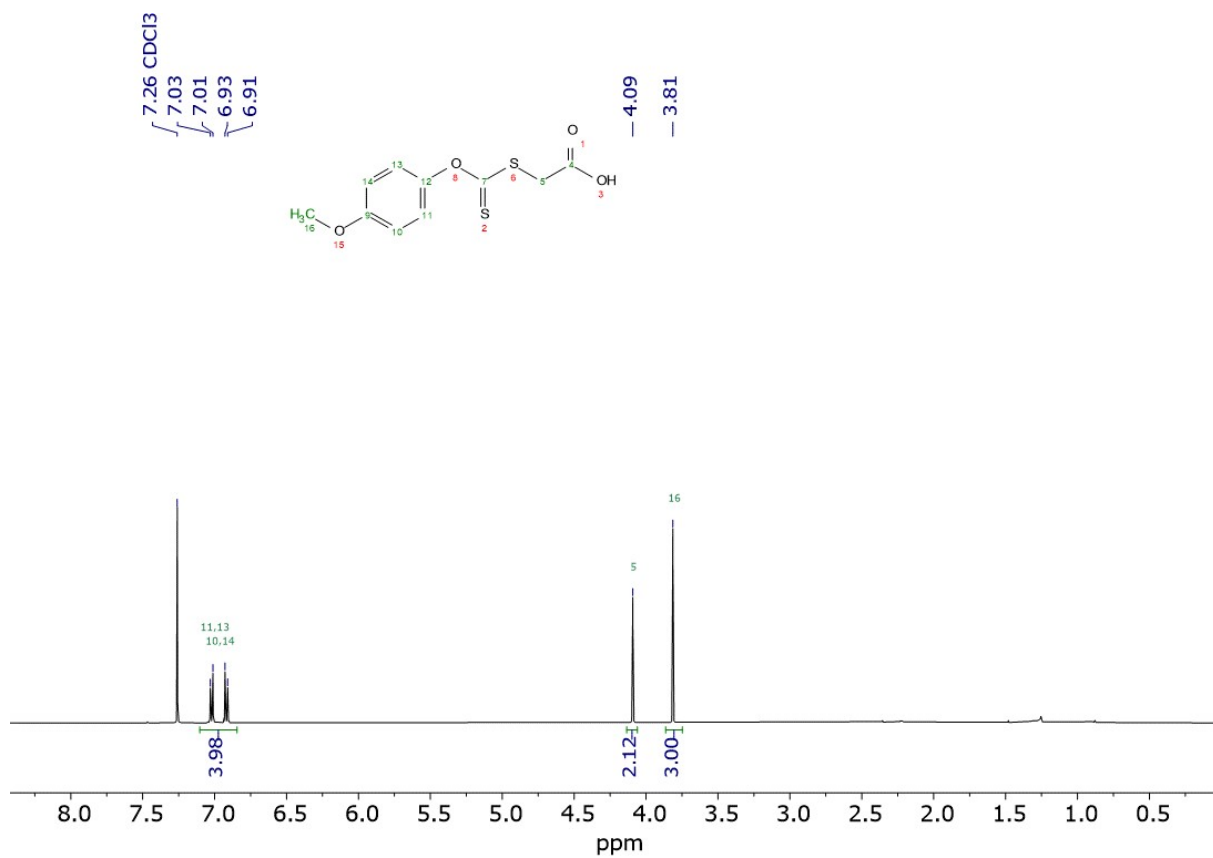


Figure S4. ¹H NMR (500 MHz, CDCl₃) spectrum of **2**.

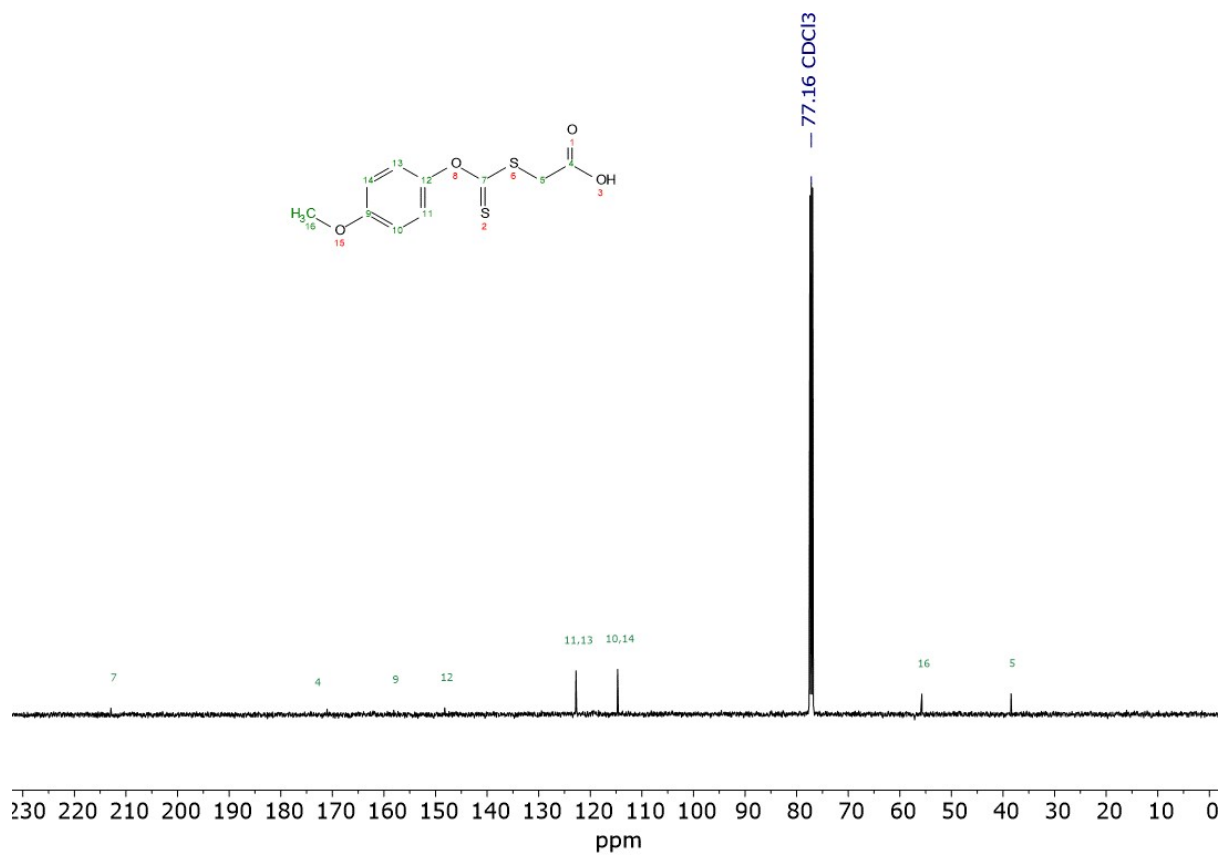


Figure S5. ¹³C NMR (125 MHz, CDCl₃) spectrum of **2**.

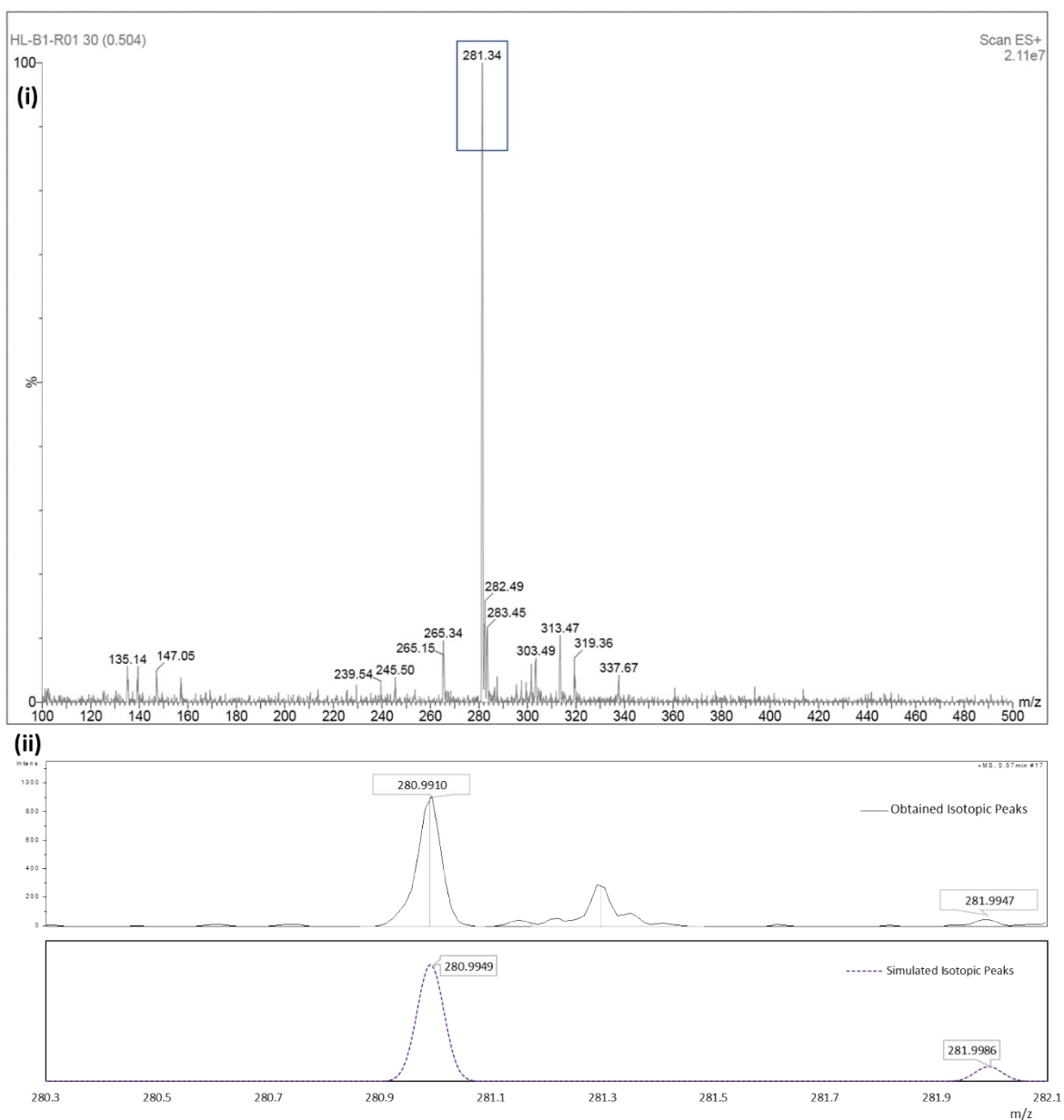


Figure S6. Mass spectroscopy of **2**. (i) shows ESI-MS spectrum. 100 % abundant species is the $[M+Na]^+$ adduct. (ii) shows HRMS $[M+Na]^+$ of **2**. Top trace shows the obtained isotopic peaks versus the simulated isotopic peaks (bottom) for $C_{10}H_{10}O_4S_2Na^+ = 280.9949$ m/z.

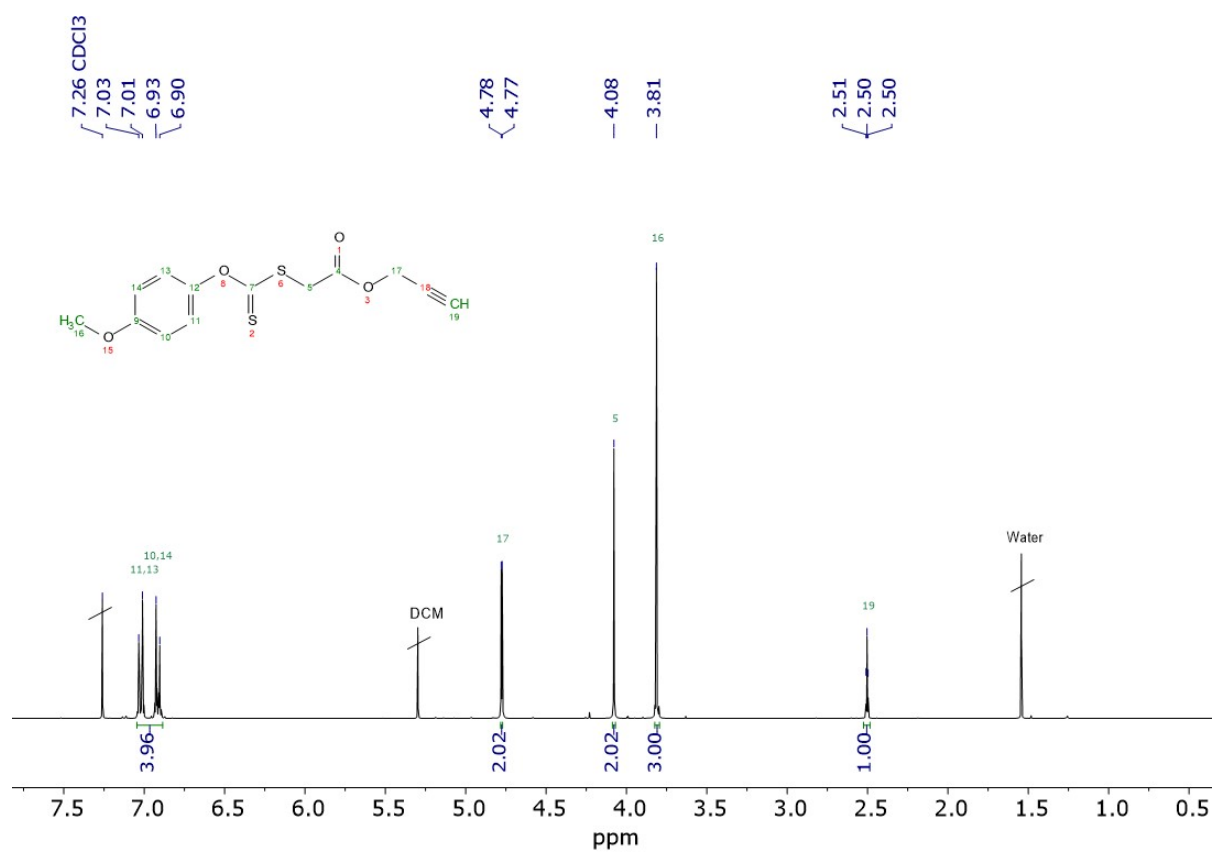


Figure S7. ¹H NMR (500 MHz, CDCl₃) spectrum of **3**.

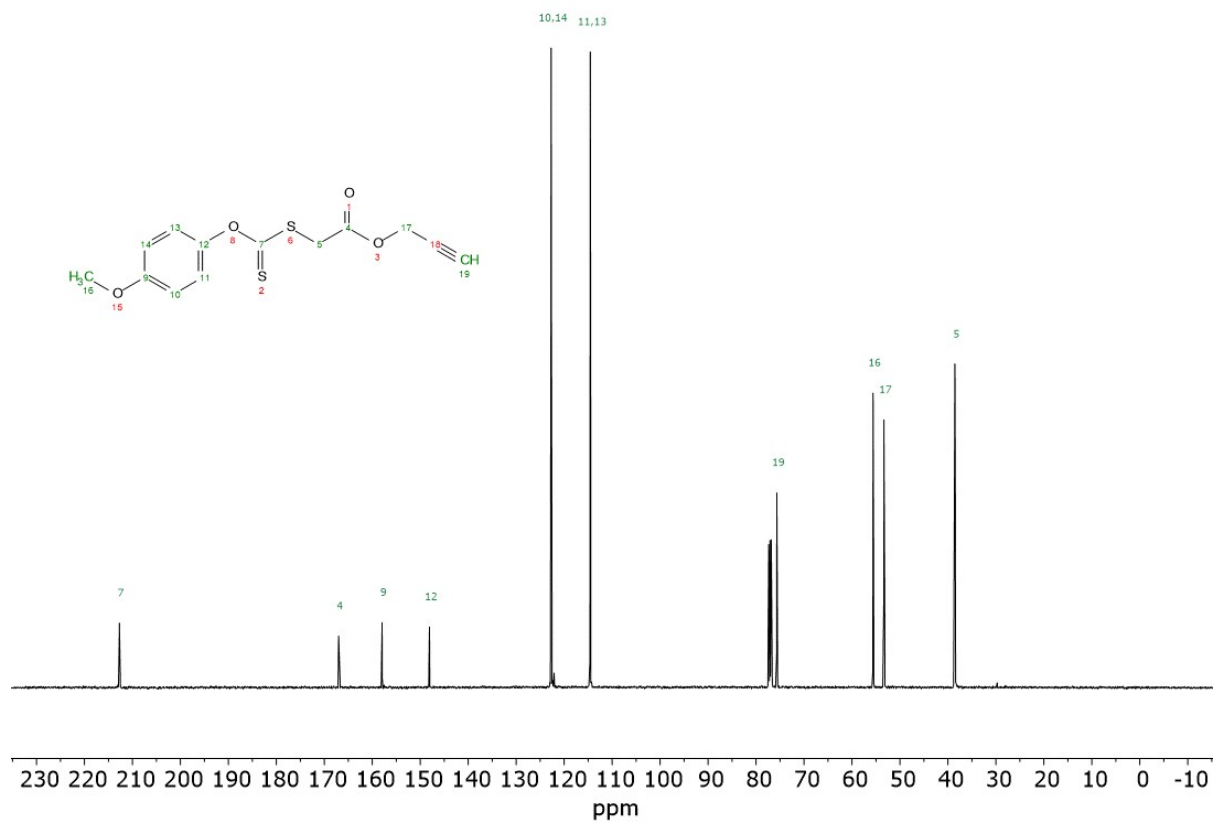


Figure S8. ¹³C NMR (125 MHz, CDCl₃) spectrum of **3**.

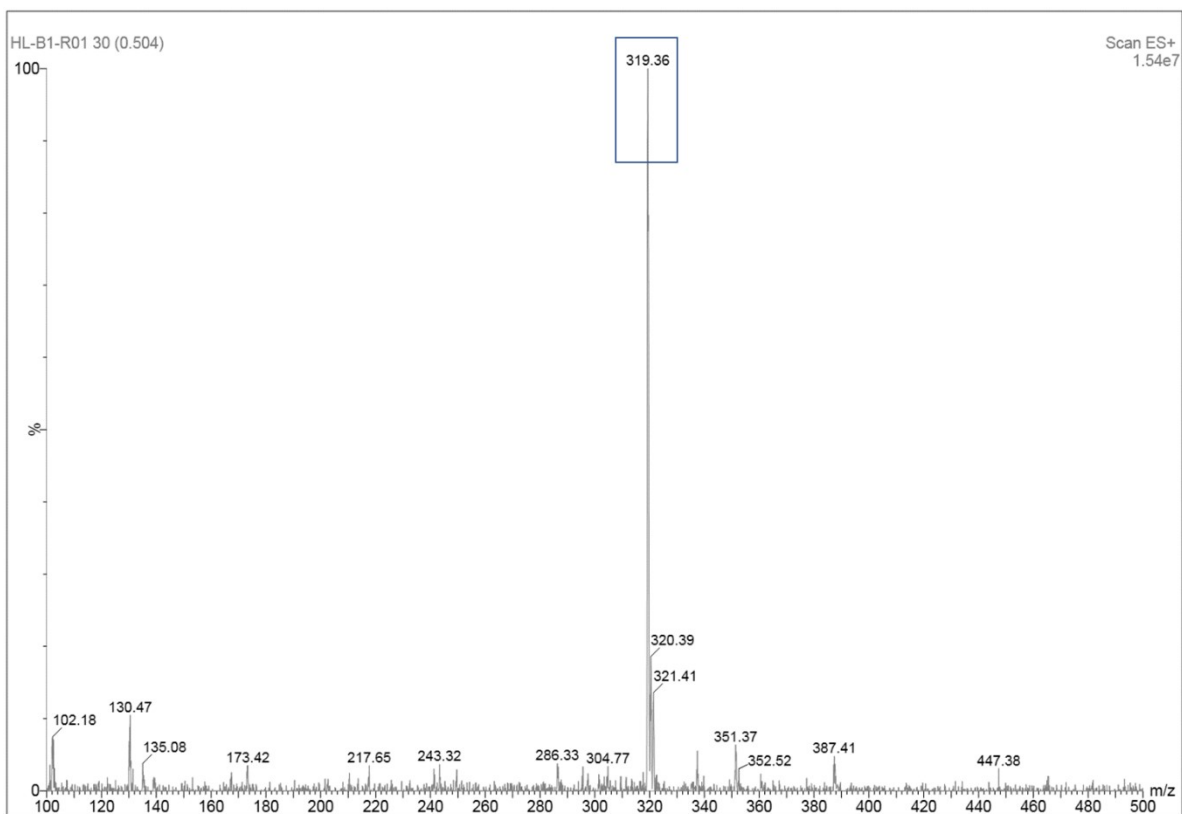


Figure S9. ESI-MS spectrum of **3**. 100 % abundant species is the $[M+Na]^+$ adduct.

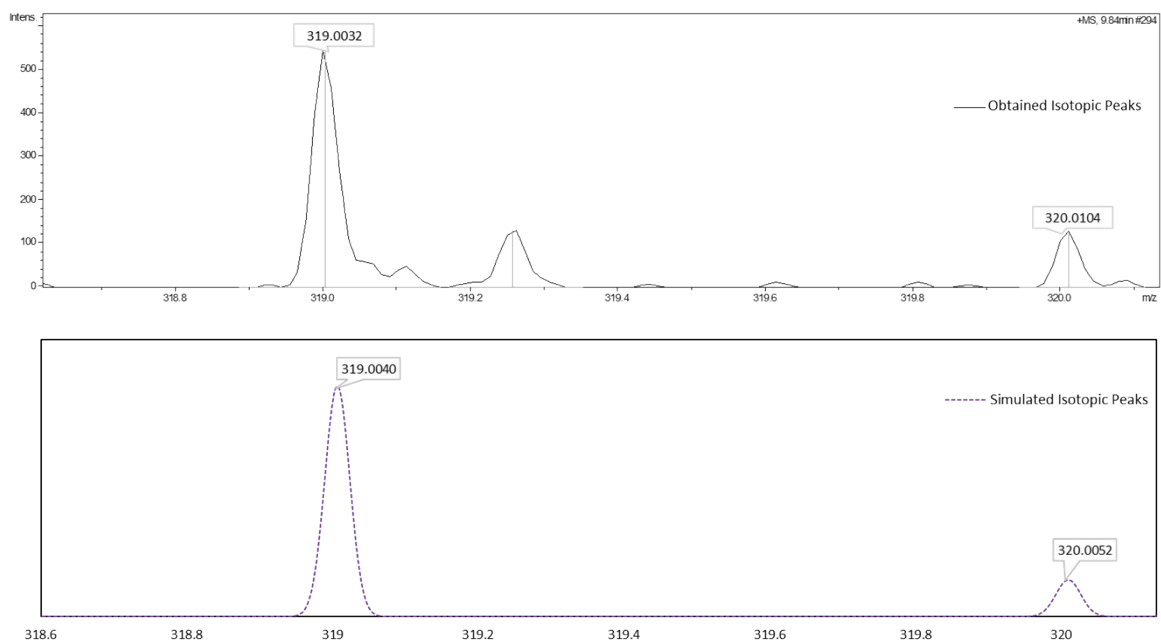


Figure S10. HRMS $[M+Na]^+$ of **3**. Top trace shows the obtained isotopic peaks versus the simulated isotopic peaks (bottom) for $C_{13}H_{12}O_4S_2Na^+ = 319.0040$ m/z.

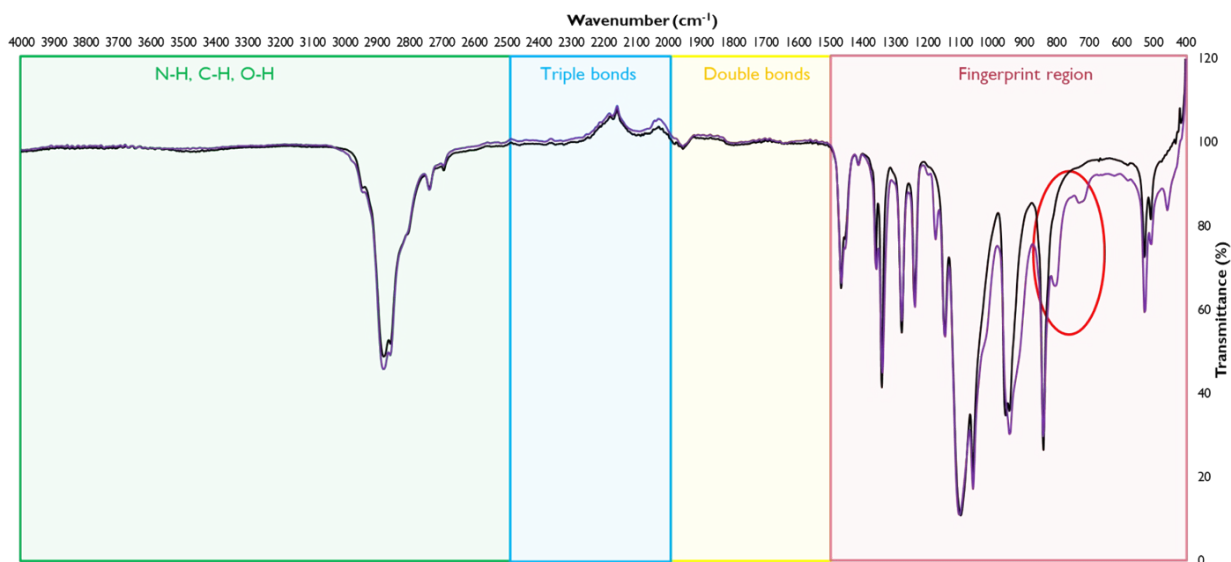


Figure S12. FT-IR spectra of MeO-PEG-OH (black) vs MeO-PEG-Oms (purple, **4**). Characteristic stretching of sulphur bonds (with oxygen and carbon) are circled in red.

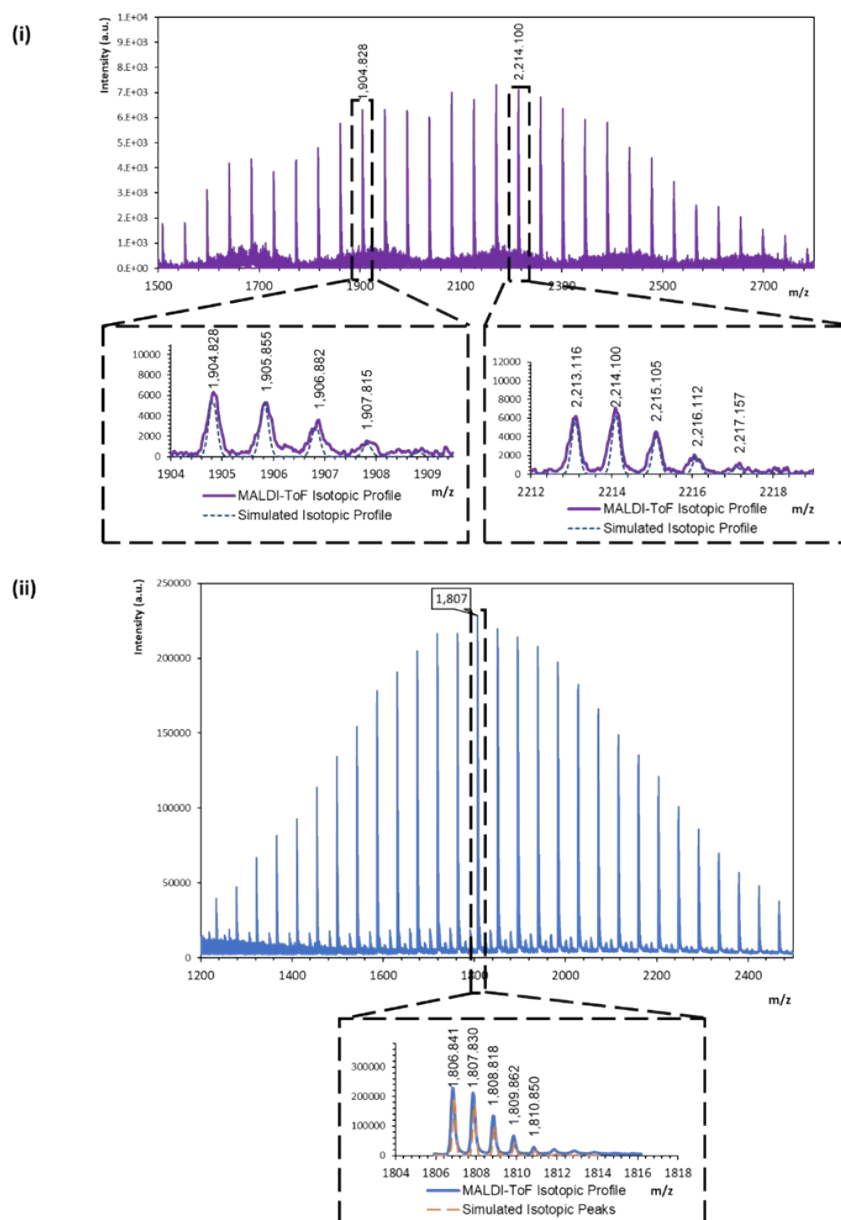


Figure S13. MALDI-ToF spectra of (i) commercially available MeO-PEG-OH. The enlargements and simulations of the highest isotopic peaks of two polymer species (different length of PEG blocks) present in the starting material are shown (empirical formula for MeO-PEG₄₁-OH; C₈₅H₁₇₂O₄₃Na⁺ = 1904.8278 m/z and MeO-PEG₄₈-OH; C₉₉H₂₀₀O₅₀Na⁺ = 2213.1157 m/z). (ii) shows MALDI-ToF spectra of MeO-PEG-OMs (**4**). Enlargement and simulation of the highest isotopic peak are shown (empirical formula for MeO-PEG₃₇-OMs; C₇₈H₁₅₈O₄₁S₁Na⁺ = 1806.8414 m/z).

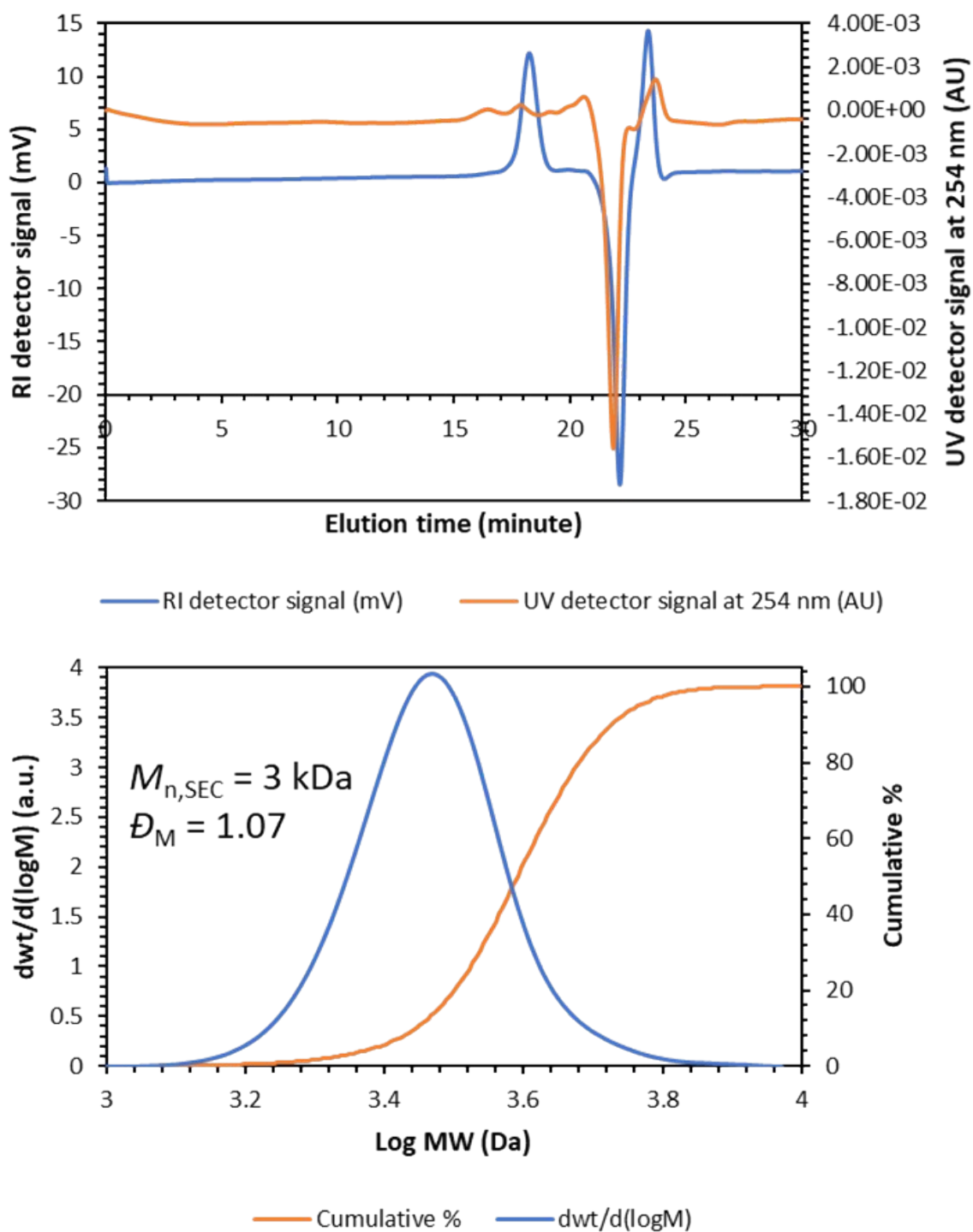


Figure S14. SEC chromatogram (THF) of MeO-PEG-OMs (4).



Figure S17. FT-IR spectra of MeO-PEG-OMs (blue, **4**) vs MeO-PEG-N₃ (green, **5**). Characteristic stretching of sulphur bonds (with oxygen and carbon in **4**) and azide (in **5**) are circled in red and purple, respectively.

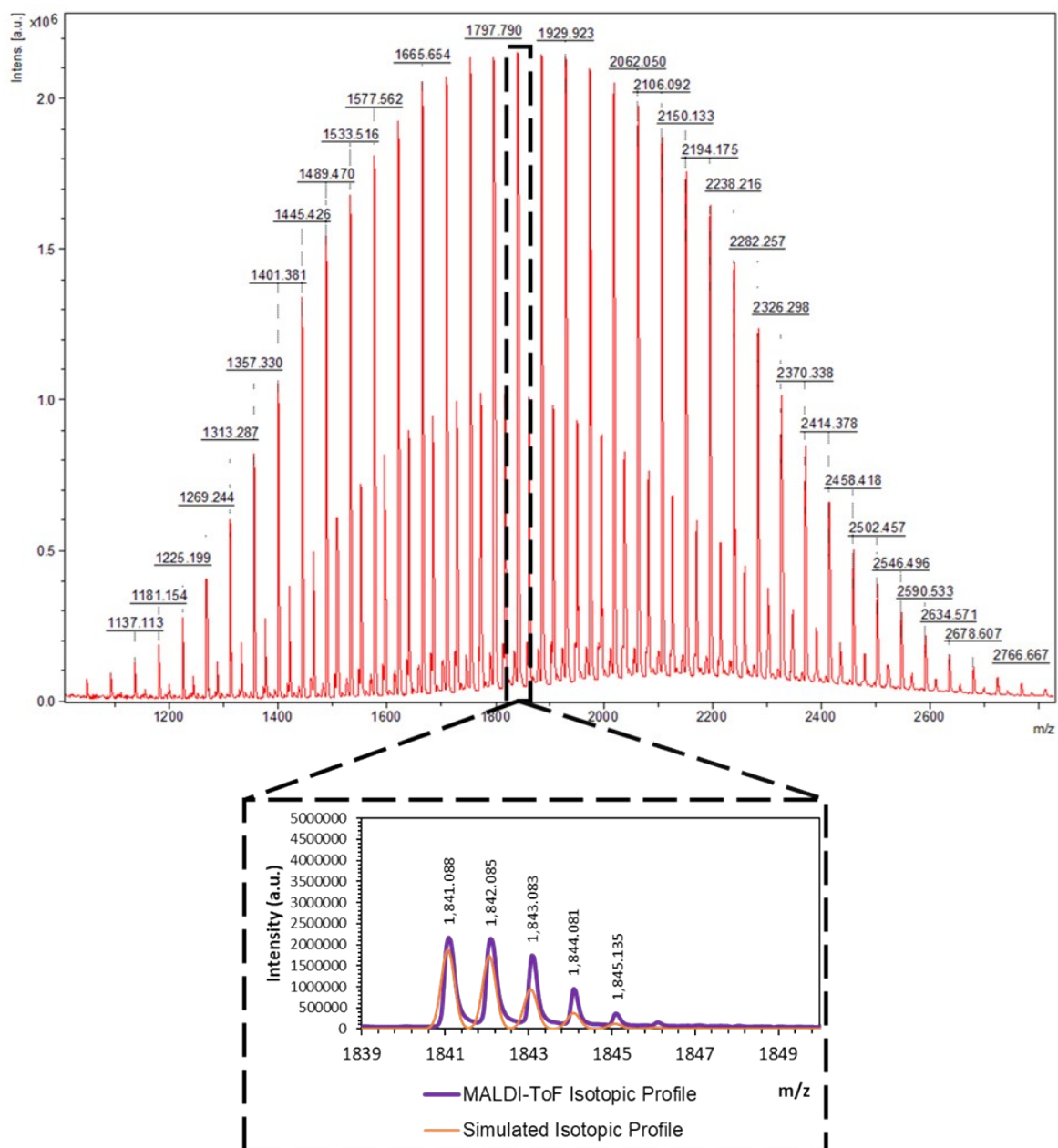


Figure S18. MALDI-ToF spectrum of azide-functional 5. Enlargement and simulation of the highest isotopic peak are shown (empirical formula for MeO-PEG₃₇-N₃; C₈₁H₁₆₃O₄₀N₃₀Na⁺ = 1841.088 m/z).

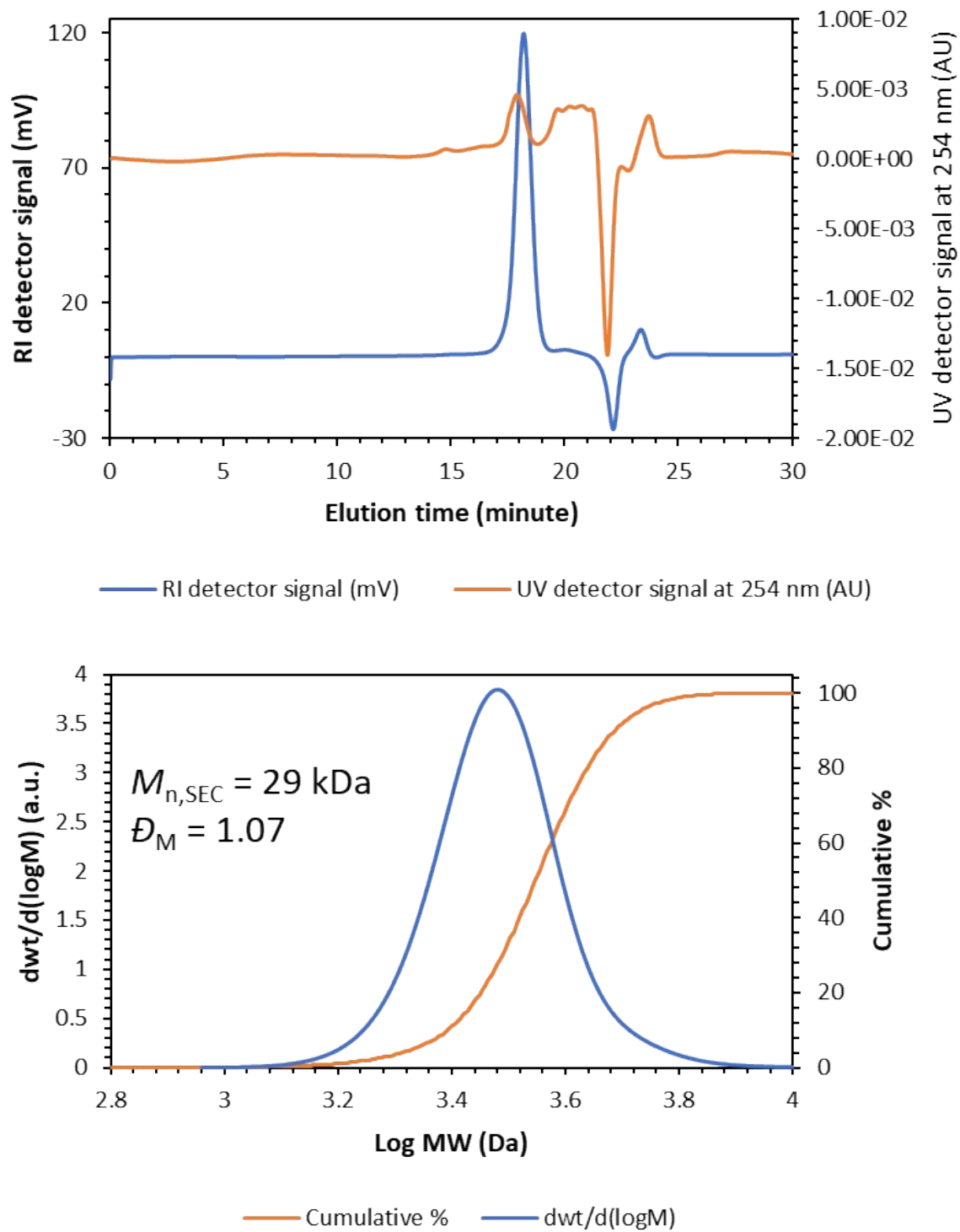


Figure S19. SEC chromatograms of azide-functional 5.

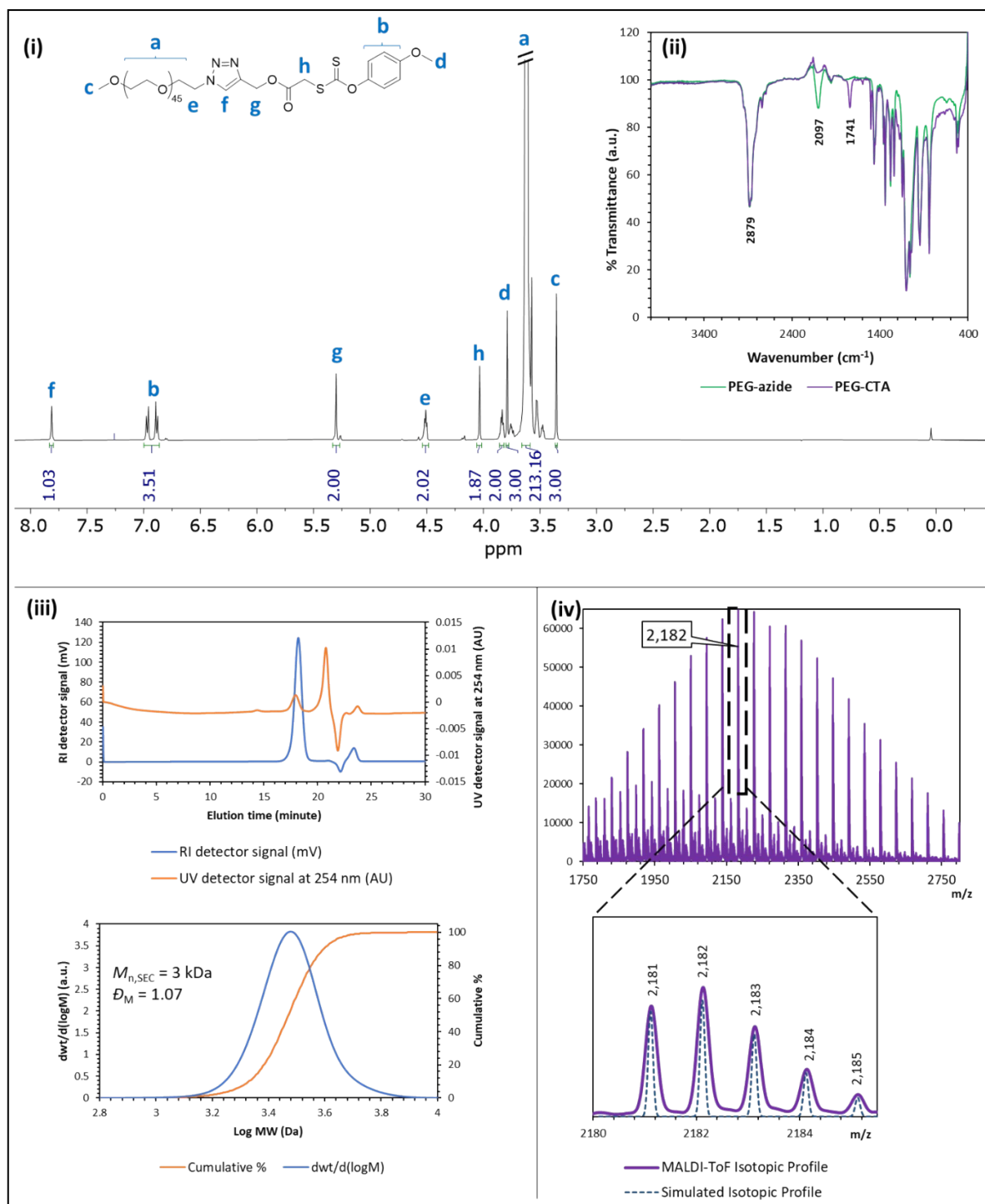


Figure S20. Characterisation data of the CuAAC 'click'-formed MeO-PEG-p-methoxyphenyl xanthate MacroCTA (**6**). Displayed spectra and chromatograms show (i) ¹H NMR spectrum, with the chemical structure, main peaks assignments and integrations, (ii) FT-IR spectra of MeO-PEG MacroCTA compared to its azide precursor, (iii) SEC chromatograms of MeO-PEG MacroCTA (**6**), with the signal from the UV detector entirely overlaps the IR detector signal, and (iv) MALDI-ToF spectrum, with enlargement and simulation of the highest isotopic peak (empirical formula for MeO-PEG40-p-methoxyphenylxantate C₉₆H₁₇₉O₄₅S₂N₃Na⁺ = 2182.117 m/z).

RAFT polymerisation of hydrophobic co-monomers using MeO-PEG macro-CTA

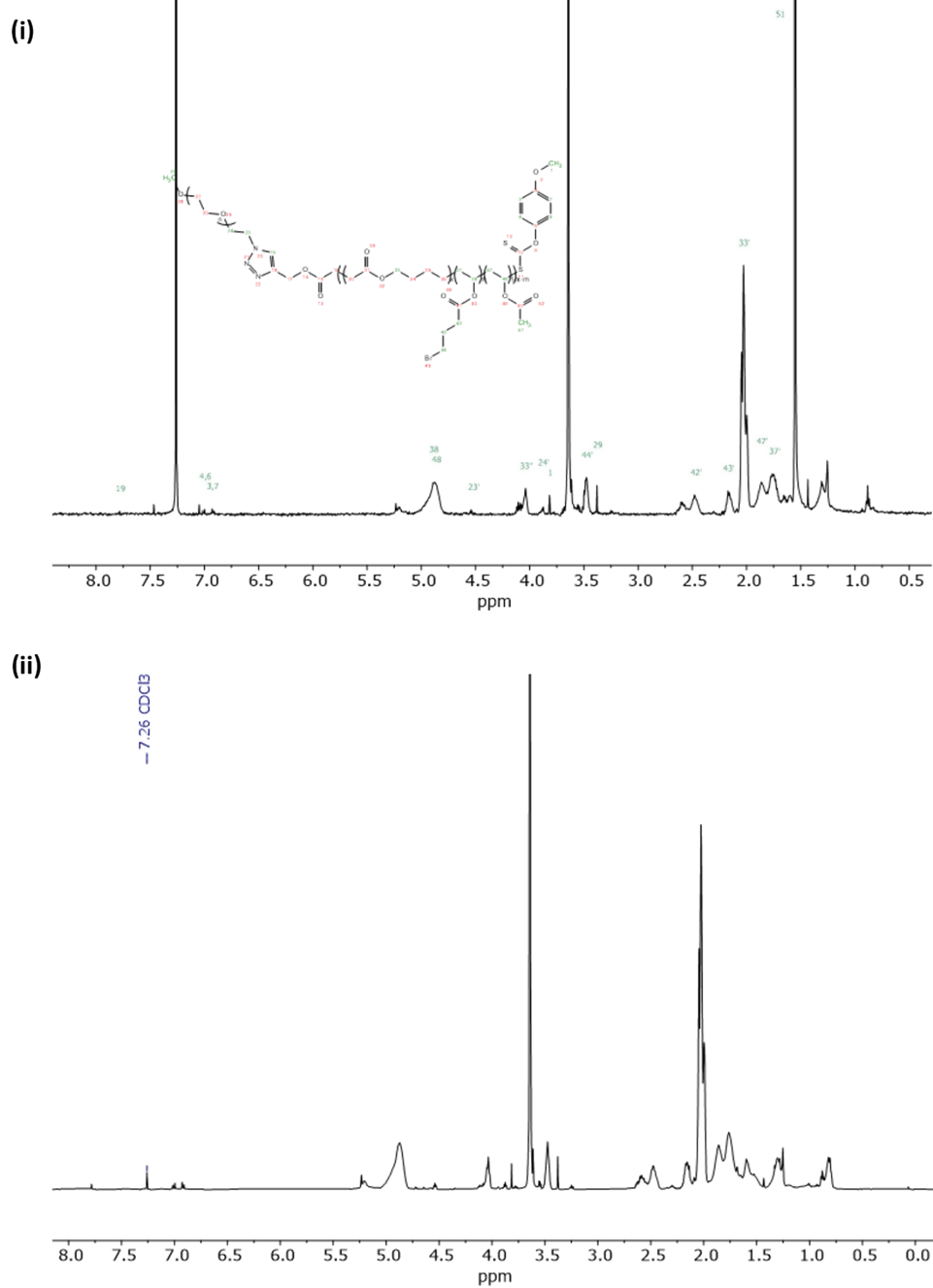


Figure S21. ^1H NMR spectrum of PEG-b-Poly(VAc-co-MDO-co-VBr); (i) **7A** and (ii) **7B**.

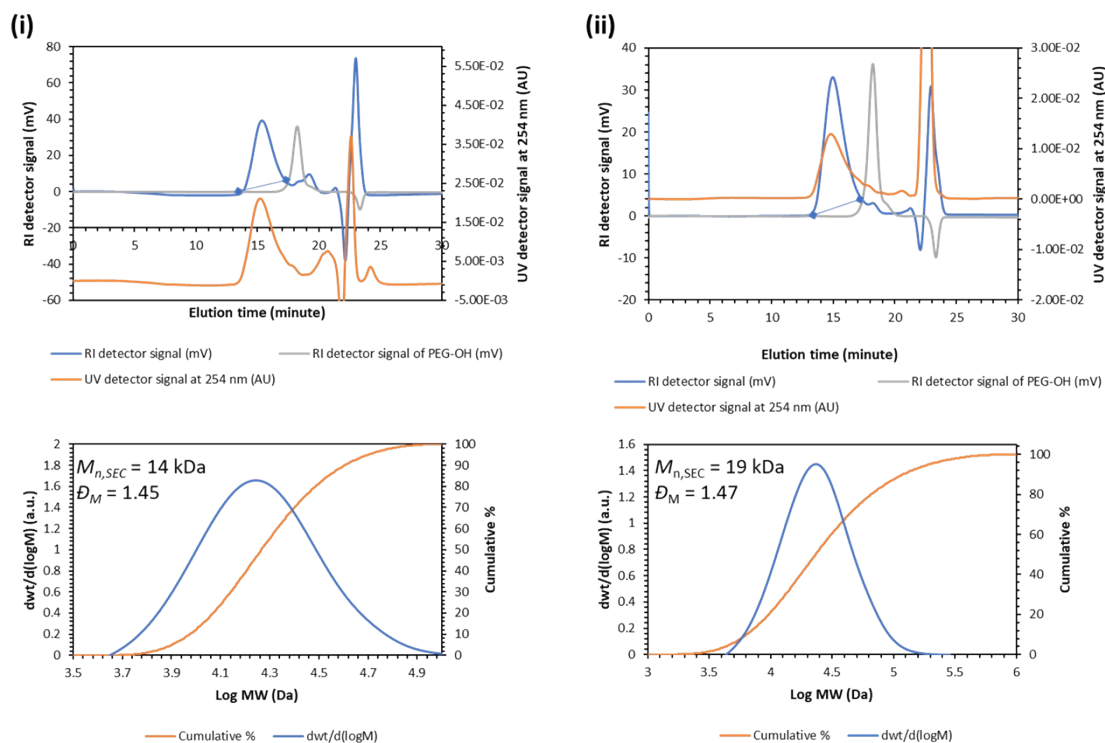


Figure S22. SEC chromatograms of PEG-b-Poly(MDO-co-VAc-co-VBr), (i) (7A), and (ii) (7B), showing monomodal dispersity of the peaks of interest. RI detector traces display a small peak eluting at 18 minutes, originating from unreacted PEG from the commercially available MeO-PEG-OH. The presence of this trace in the starting material was confirmed using MALDI-ToF, as in Figure S-13(i). Extra purification was not considered at this stage to keep the yield high, as these traces (<2kDa) are ultimately purified in the dialysis step using 10K MWCO dialysis tubing following the formation of NP.

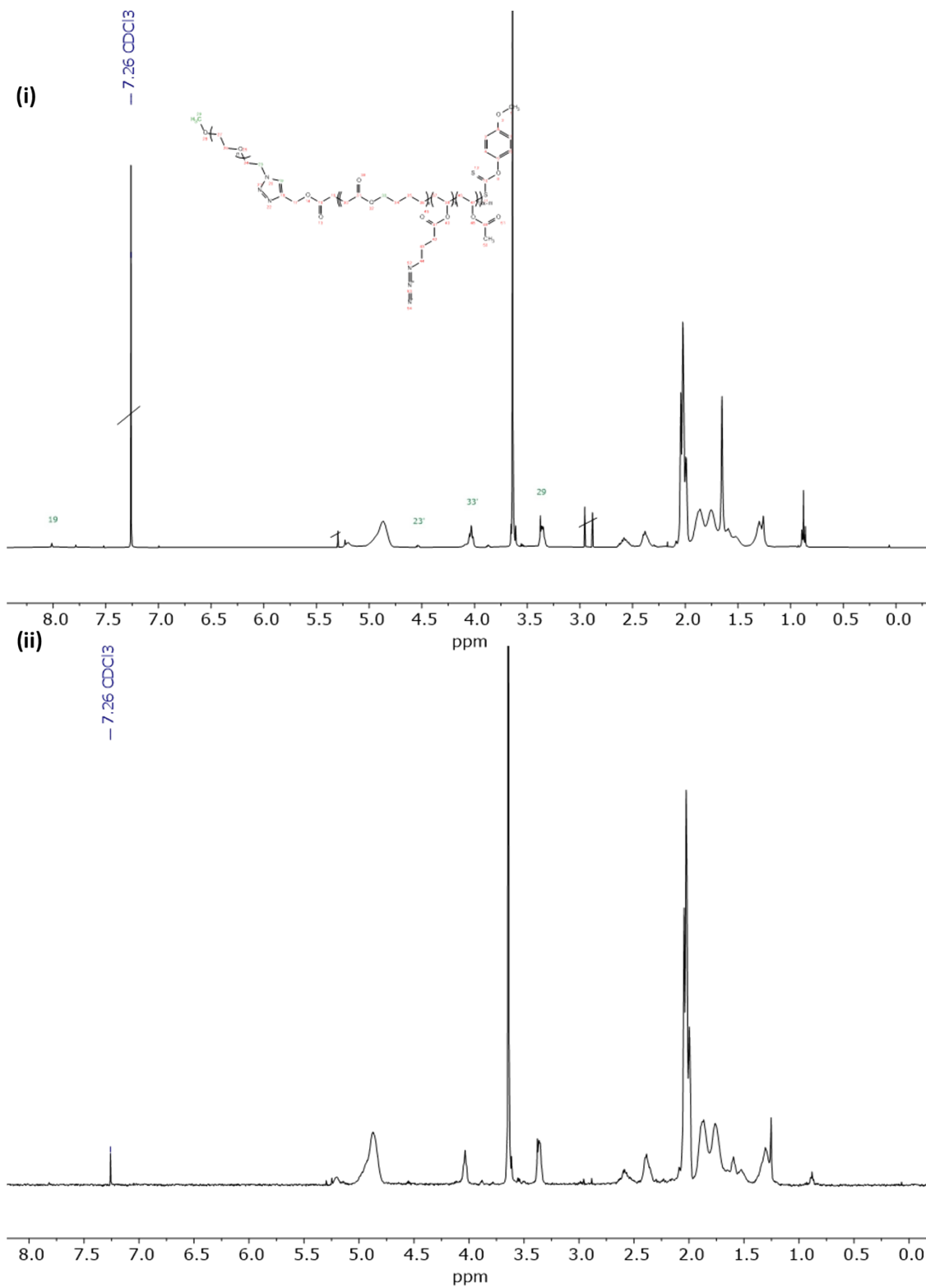


Figure S23. ¹H NMR spectrum of PEG-b-Poly(VAc-co-MDO-co-(VN₃)); (i) **8A** and (ii) **8B**.

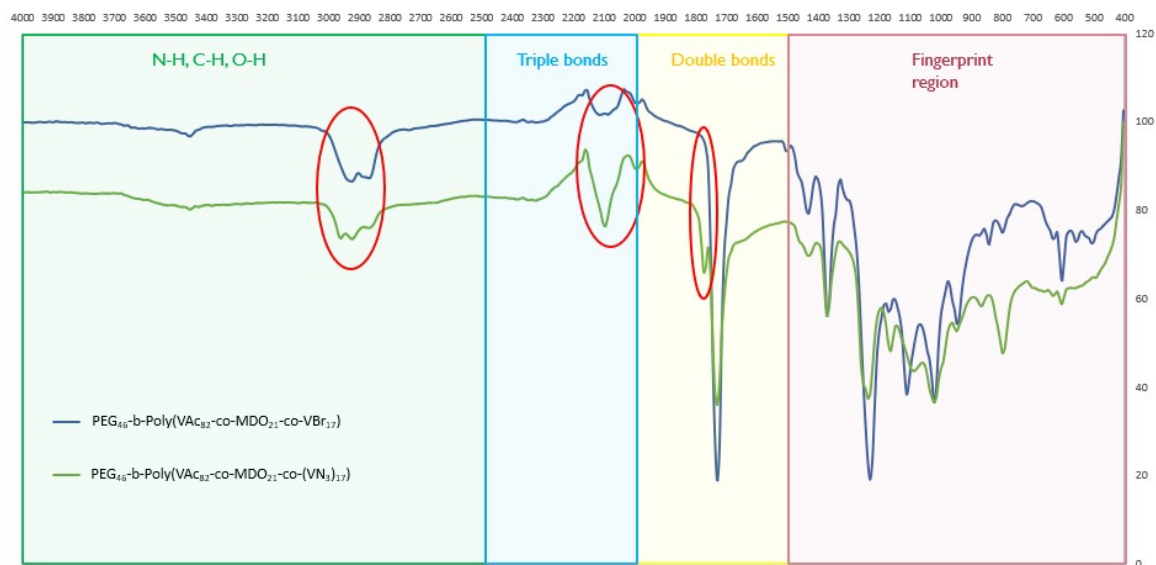


Figure S24. FT-IR spectra of PEG-b-Poly(MDO-co-VAc-co-VBr); (**7A**, blue) vs PEG-b-Poly(MDO-co-VAc-co-(VN₃)); (**8A**, green).

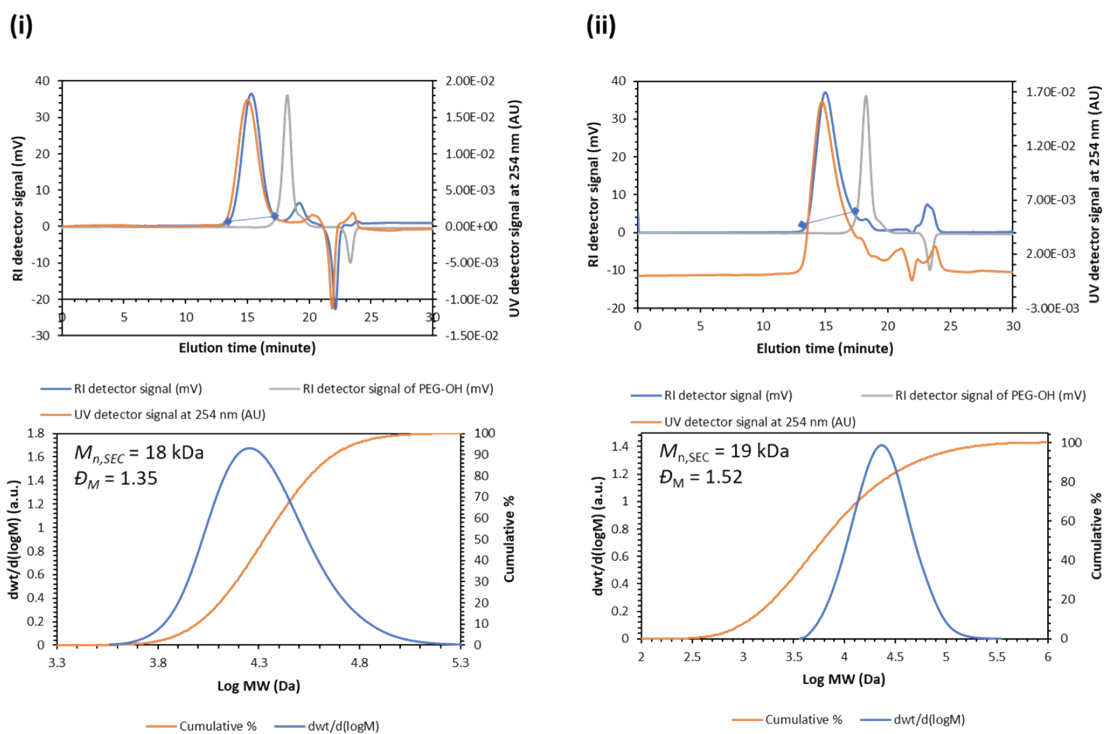


Figure S25. SEC chromatograms of PEG-b-Poly(MDO-co-VAc-co-(VN₃)), (i) **8A** and (ii) **8B**, showing monomodal dispersities of the peaks of interest. RI detector traces display a small peak eluting at 18 minutes, originating from unreacted PEG from the commercially available MeO-PEG-OH. The presence of this trace in the starting material was confirmed using MALDI-ToF, as in Figure S-13(i). Extra purification was not considered at this stage to keep the yield high, as these traces (<2kDa) are ultimately purified in the dialysis step using 10K MWCO dialysis tubing following the formation of NP.

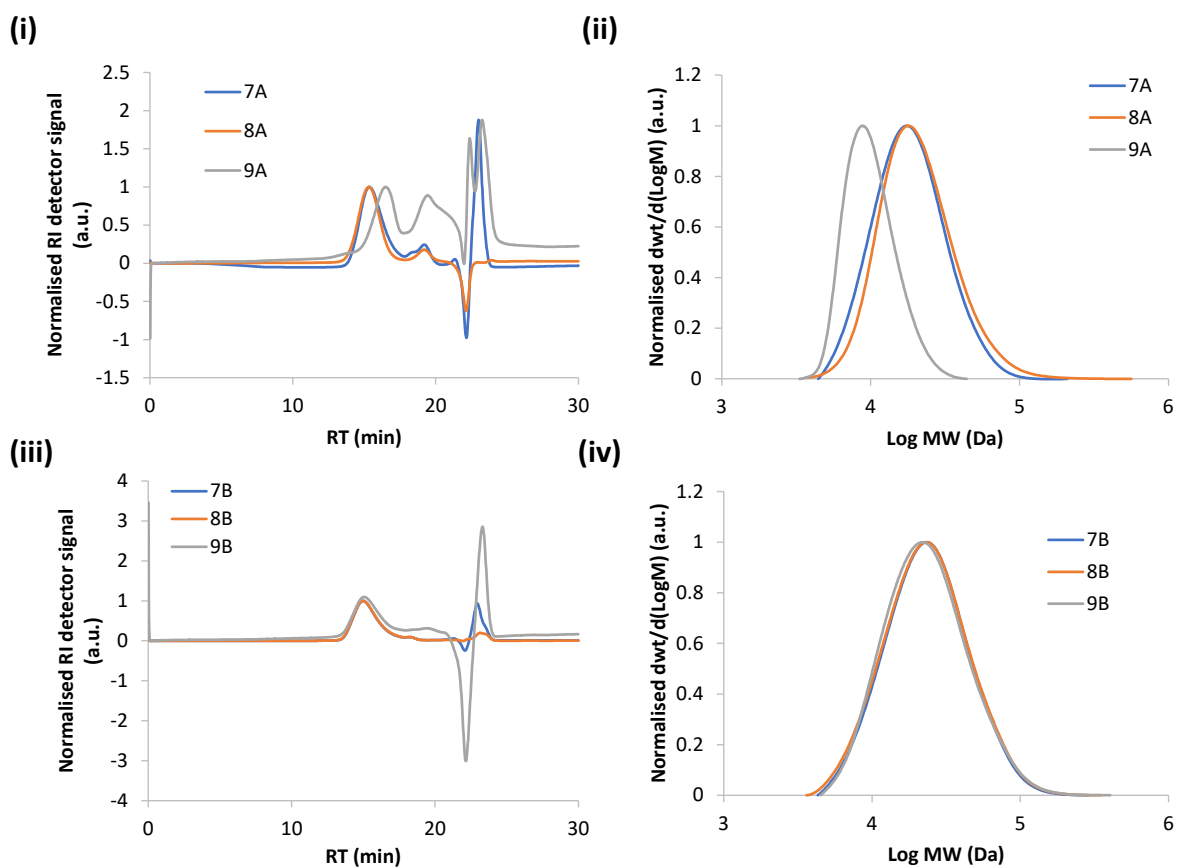


Figure S26. Comparison of the SEC chromatograms of PEG-b-Poly(MDO-co-VAc-co-VBr) (7A and B), PEG-b-Poly(MDO-co-VAc-co-VN₃) (8A and B), and PEG-b-Poly(MDO-co-VAc-co-VN₃-co-VCy5) (9A and B). (i) Normalised raw RI data for "A" series, (ii) Normalised log weight distribution for "A" series, (iii) Normalised raw RI data for "B" series, and (iv) Normalised log weight distribution for "B" series.

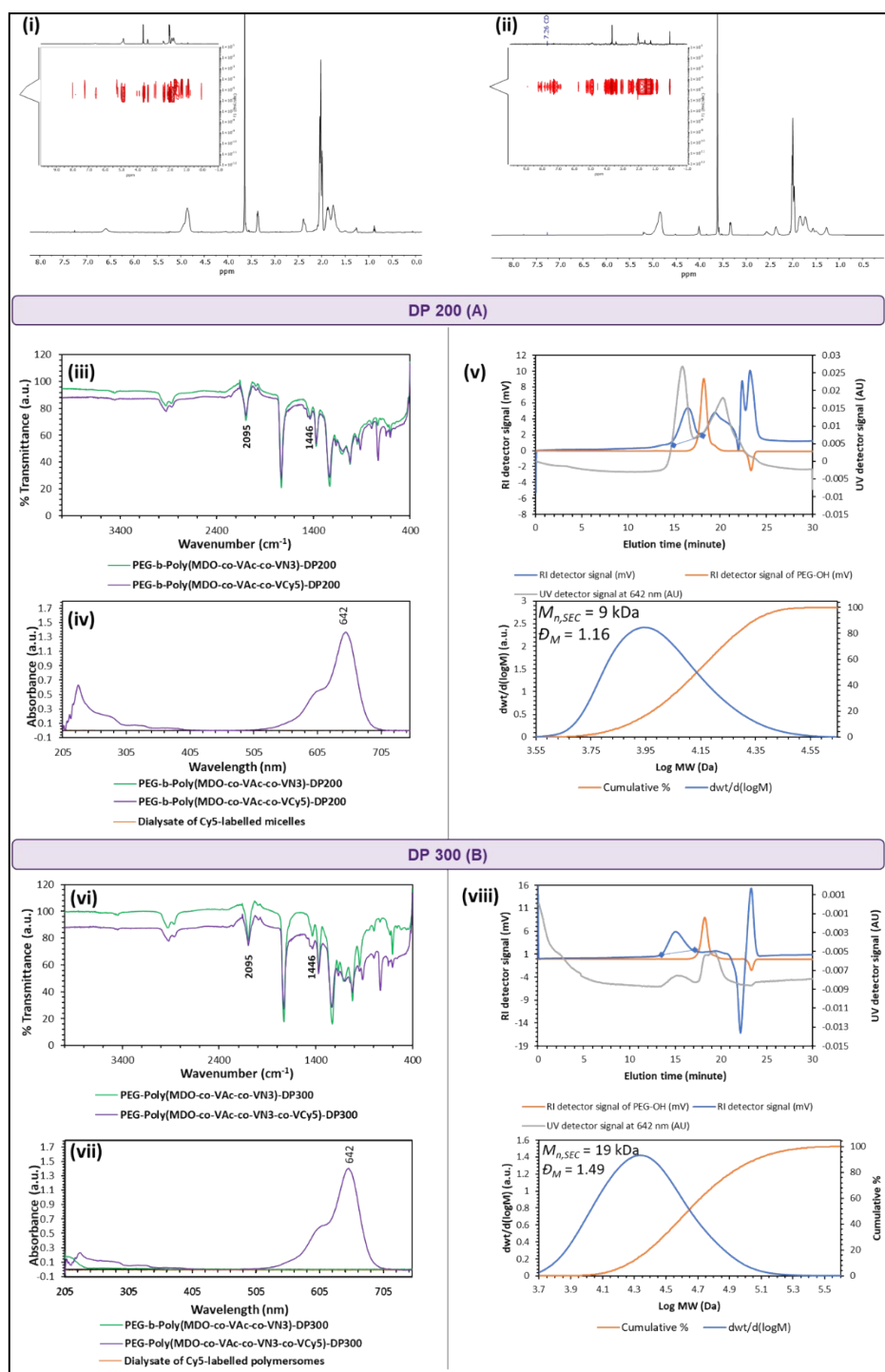


Figure S27. Main characterisation data of **9A** and **9B**. ^1H NMR spectra (i) and (ii) show Cy5-labelled blocks, **9A** and **9B**, respectively. Insets show polymer diffusion as one band in 2D DOSY NMR, confirming the successful conjugation of Cy5-DBCO to the polymer chains. (iii) and (vi) show FT-IR spectra of non-labelled (green, **8A** and **8B**) and Cy5-labelled (magenta, **9A** and **9B**) polymers, respectively. (iv) and (vii) show UV-Vis spectra of non-labelled (green, **8A** and **8B**) and Cy5-labelled (magenta, **9A** and **9B**) polymers, respectively. (v) and (viii) show GPC/SEC spectra of **9A** and **9B**, respectively, as recorded by UV detectors (at 642) and RI detector. RI detector traces display a small peak eluting at 18 minutes, originating from unreacted PEG from the commercially available MeO-PEG-OH, as confirmed when overlaying the orange RI trace of the latter with the RI traces of **9A** and **9B**. Extra purification was not considered at this stage to keep the yield high, as these traces (<2kDa) are ultimately purified in the dialysis step using 10K MWCO dialysis tubing following the formation of NP.

Cmc determination and self-assembly of the amphiphilic copolymers

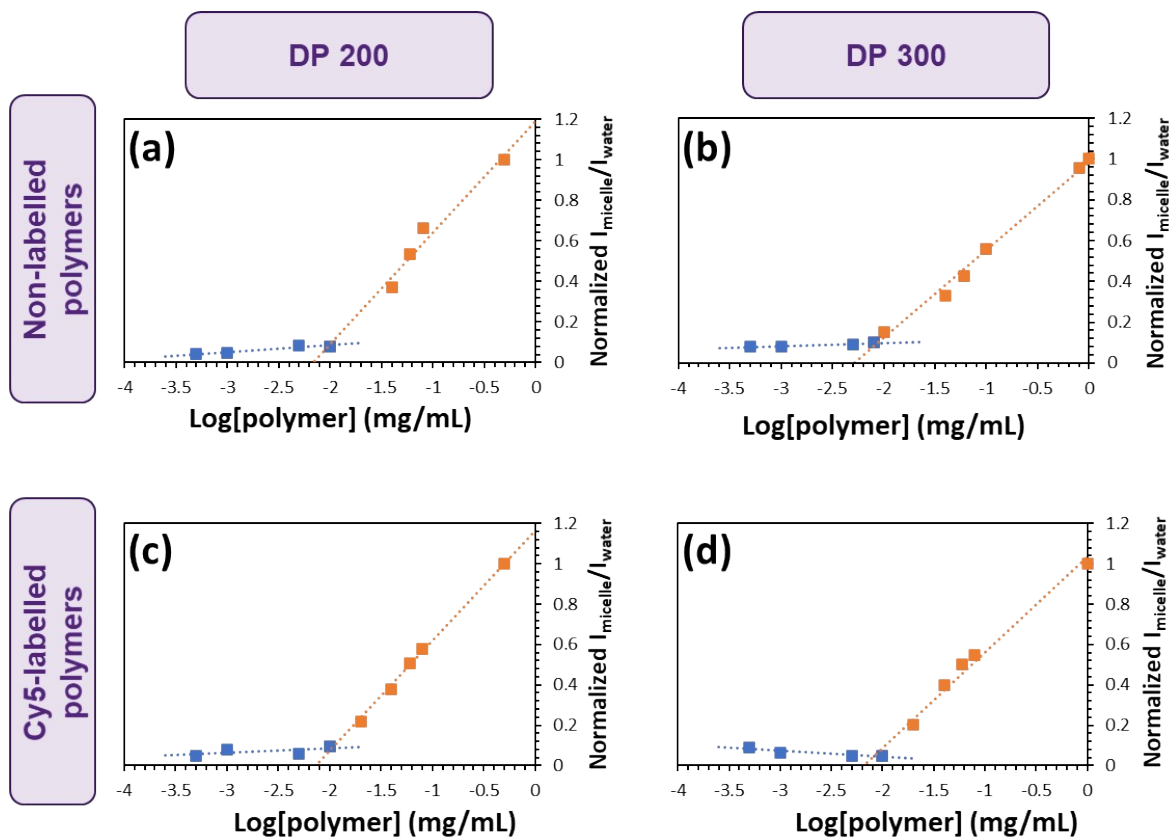


Figure S28. cmc determination of the RAFT-polymerised co-polymers synthesized at different functionalities and degrees of polymerisation. $(I_{\text{micelle}}/I_{\text{water}})$ versus (log polymer concentration) plots indicate the change of PNA fluorescent intensity as the polymer concentrations change. The intercepts between low (blue) and high (orange) concentration regions correspond to the cmc values of each polymer, where the sharp increment in $I_{\text{micelle}}/I_{\text{water}}$ indicate the formation of micelles. cmc is investigated for non-labelled (a) PEG-*b*-Poly(MDO-*co*-VAc-*co*-VN₃); (**8A**) and (b) PEG-*b*-Poly(MDO-*co*-VAc-*co*-VN₃); (**8B**), or Cy5-labelled (c) PEG-*b*-Poly(MDO-*co*-VAc-*co*-VN₃-*co*-VCy5); (**9A**) and (d) PEG-*b*-Poly(MDO-*co*-VAc-*co*-VN₃-*co*-VCy5); (**9B**) di-block copolymers.

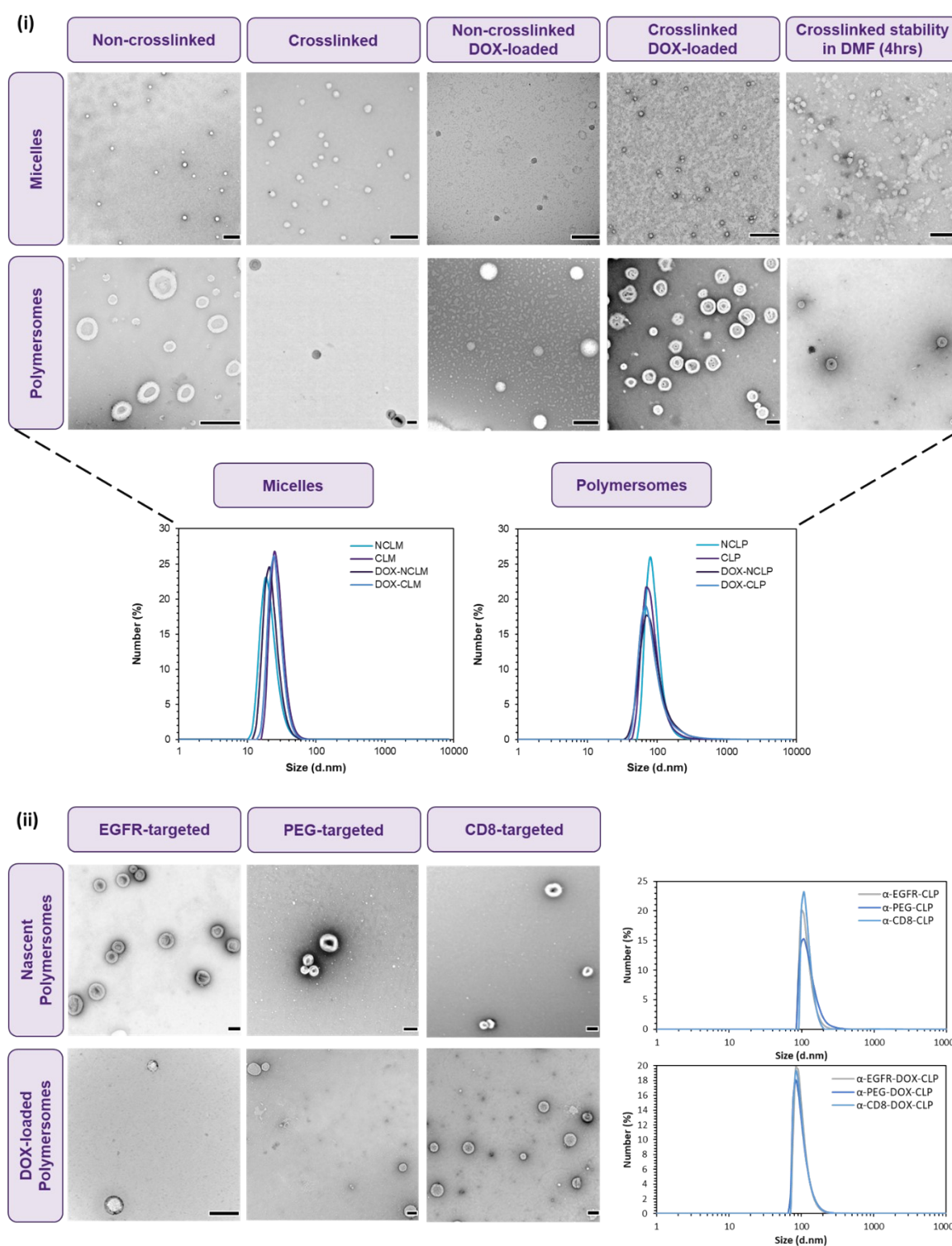


Figure S29. TEM images and DLS frequency curves (number %) of: (i) DOX-loaded or nascent, crosslinked, or non-crosslinked micelles and polymersomes. Images of crosslinked NPs following 4 hours of incubation in DMF are also shown, where both aggregates efficiently maintain their morphologies; and (ii) DOX-loaded or nascent polymersomes conjugated to α EGFR- α PEG, α PEG- α PEG, or α CD8- α PEG BsAb. TEM and DLS analysis confirm that the conjugation of different BsAbs used in this work does not change the size nor the morphology of our NP. The scalebars correspond to 200 nm in all images.

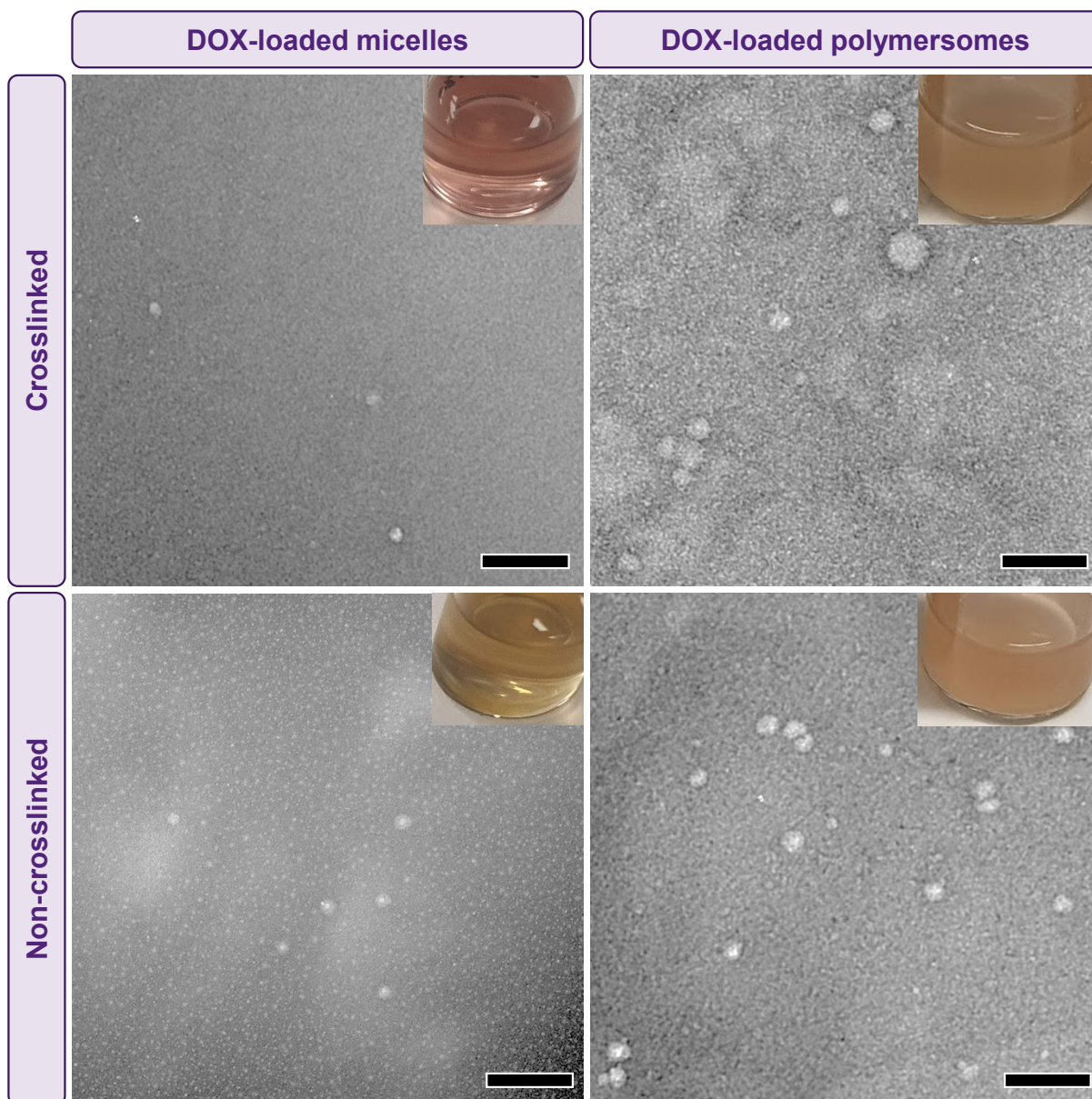


Figure S30. Dissociation of DOX-loaded, crosslinked or non-crosslinked micelles and polymersomes, incubated for 15 days in FBS serum containing 50% media, as observed by TEM. TEM images show NP morphologies following 4 days of incubation. Scalebars correspond to 100 nm in all the images. Insets show the NP vials at the end of the incubation period, where the pH has turned acidic (phenol turned orange/yellowish).

In vitro cellular association and uptake studies

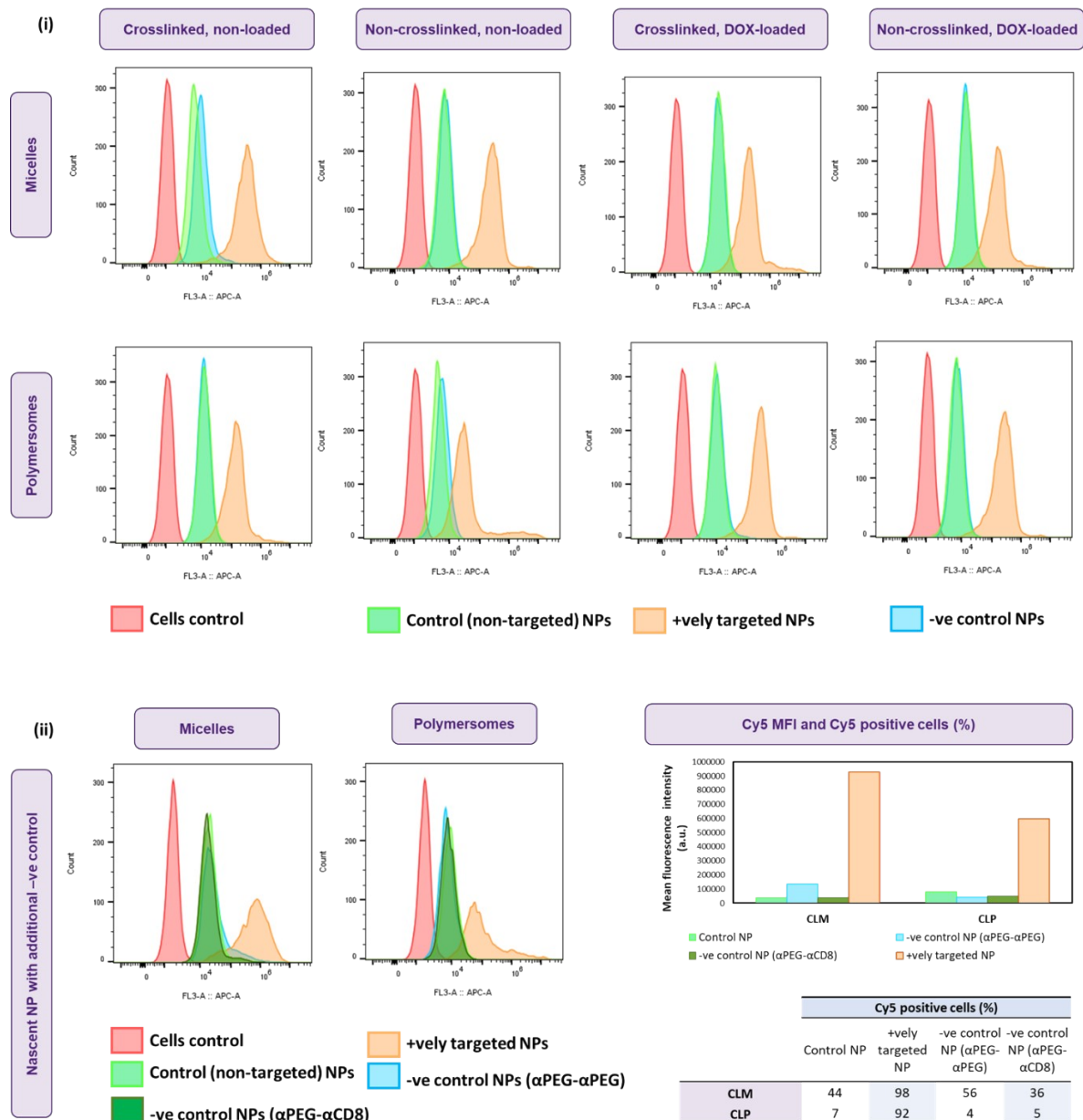


Figure S31. Cellular uptake of nascent or DOX-loaded, crosslinked or non-crosslinked, targeted or control micelles or polymersomes in MDA-MB-468 cancer cells. (i) shows results observed 1-hour post-treatment with NPs, at 37°C. Brown histograms represent MFI values for cells treated with EGFR-targeted NPs, whereas blue and green histograms represent MFI values of cells treated with negative controls (conjugated to α -PEG- α -PEG BsAbs) and control (non-targeted) NPs, respectively. (ii) shows results observed four hours post-treatment with nascent NPs, at 37°C. Brown histograms represent MFI values for cells treated with EGFR-targeted NPs, whereas blue, dark-green and green histograms represent MFI values of cells treated with negative controls (conjugated to α PEG- α PEG and α PEG- α CD8 BsAbs) and control (non-targeted) NPs, respectively. The blue and dark-green histograms of the negative controls demonstrate similar uptake to the non-targeted NPs, when either α PEG- α PEG or α PEG- α CD8 BsAbs were conjugated with our NPs, as summarised numerically in the table. This indicates that either of these BsAbs could be used with our systems to represent the -ve control group, even for longer duration of treatment with NPs.

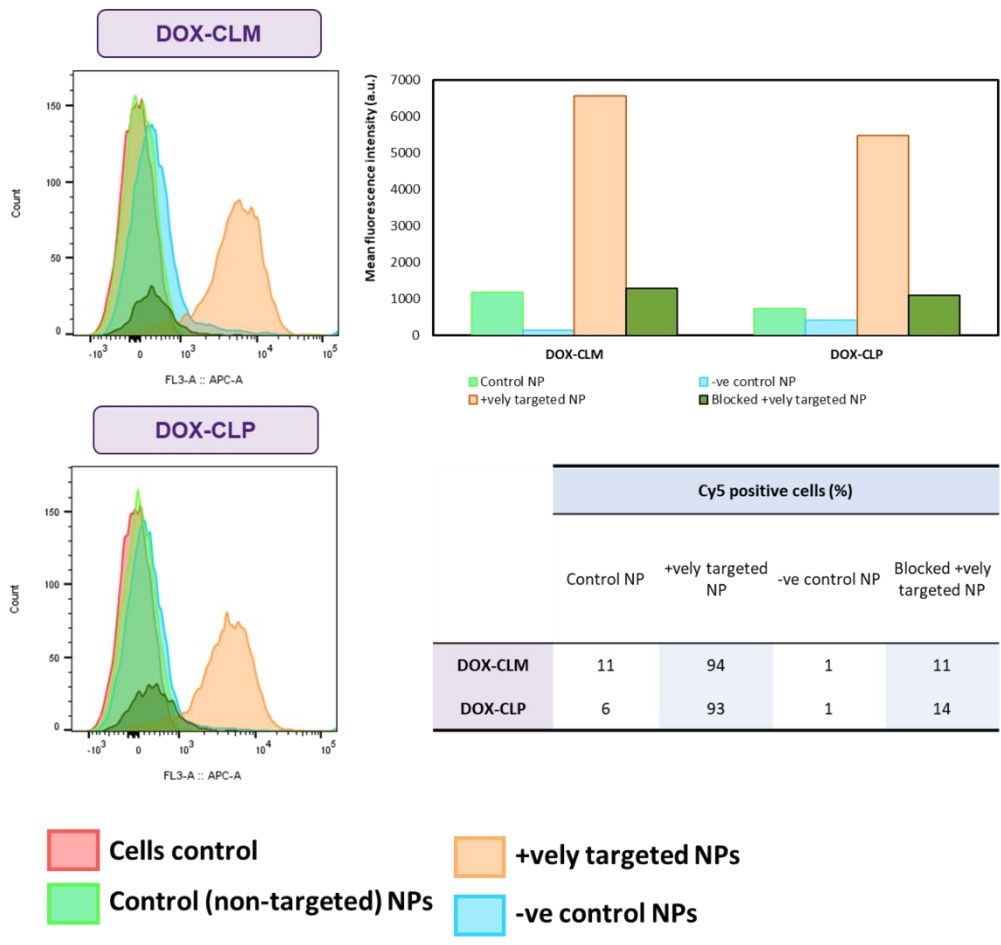


Figure S32. Cellular uptake of crosslinked, DOX-loaded, targeted and control micelles and polymersomes in MDA-MB-468 cancer cells, compared to targeted NP interrogated against MDA-MB-468 cells with blocked EGFR. Results observed four-hours post-treatment with NP, at 37°C. Brown histograms represent MFI values for cells treated with EGFR-targeted NP, whereas blue and green histograms represent MFI values of cells treated with negative controls (conjugated to α -PEG- α -PEG BsAb) and control (non-targeted) NP, respectively. MFI values for blocked cells treated with EGFR-targeted NP are shown in dark green.

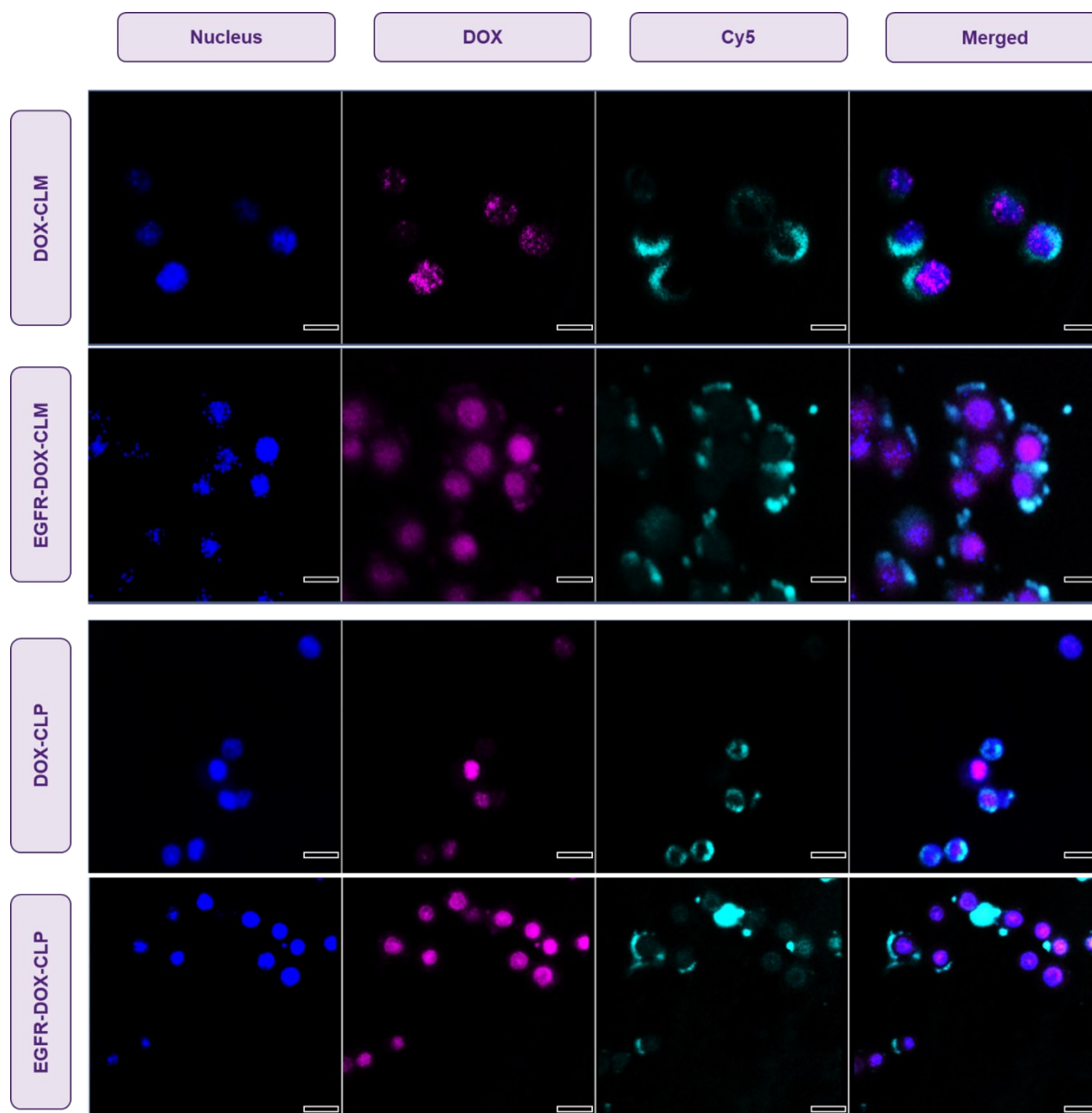


Figure S33. Representative CLSM micrographs of MDA-MB-468 live cells treated with DOX-loaded NP. Treatment groups (DOX concentration in each is $10 \mu\text{g mL}^{-1}$) were either EGFR-targeted or non-targeted (control) micelles or polymersomes. Cells were imaged five hours post exposure to treatment, before using Hoechst 33342 method to stain the nuclei and detect apoptosis. For each panel, the images show stained nuclei (blue), DOX fluorescence (magenta), NP (Cy5) fluorescence (cyan), and overlaid representation of the three channels (from left to right). Scalebars denote $20 \mu\text{m}$ in all the images.

Minimum Information Reporting in Bio–Nano Experimental Literature Checklist

The MIRIBEL guidelines were introduced here: <https://doi.org/10.1038/s41565-018-0246-4>

The development of these guidelines was led by the ARC Centre of Excellence in Convergent BioNano Science and Technology: <https://www.cbns.org.au/>. Any updates or revisions to this document will be made available here: <http://doi.org/10.17605/OSF.IO/SMVTF>. This document is made available under a CC-BY 4.0 license: <https://creativecommons.org/licenses/by/4.0/>.

The MIRIBEL guidelines were developed to facilitate reporting and dissemination of research in bio–nano science. Their development was inspired by various similar efforts:

- MIAME (microarray experiments): *Nat. Genet.* **29** (2001), 365; <http://doi.org/10.1038/ng1201-365>
- MIRIAM (biochemical models): *Nat. Biotechnol.* **23** (2005) 1509; <http://doi.org/10.1038/nbt1156>
- MIBBI (biology/biomedicine): *Nat. Biotechnol.* **26** (2008) 889; <http://doi.org/10.1038/nbt.1411>
- MIGS (genome sequencing): *Nat. Biotechnol.* **26** (2008) 541; <http://doi.org/10.1038/nbt1360>
- MIQE (quantitative PCR): *Clin. Chem.* **55** (2009) 611; <http://doi.org/10.1373/clinchem.2008.112797>
- ARRIVE (animal research): *PLOS Biol.* **8** (2010) e1000412; <http://doi.org/10.1371/journal.pbio.1000412>
- *Nature's* reporting standards:
 - o Life science: <https://www.nature.com/authors/policies/reporting.pdf>; e.g., *Nat. Nanotechnol.* **9** (2014) 949; <http://doi.org/10.1038/nnano.2014.287>
 - o Solar cells: <https://www.nature.com/authors/policies/solarchecklist.pdf>; e.g., *Nat. Photonics* **9** (2015) 703; <http://doi.org/10.1038/nphoton.2015.233>
 - o Lasers: <https://www.nature.com/authors/policies/laserchecklist.pdf>; e.g., *Nat. Photonics* **11** (2017) 139; <http://doi.org/10.1038/nphoton.2017.28>
- The “TOP guidelines”: e.g., *Science* **352** (2016) 1147; <http://doi.org/10.1126/science.aag2359>

Similar to many of the efforts listed above, the parameters included in this checklist are **not** intended to be definitive requirements; instead they are intended as ‘points to be considered’, with authors themselves deciding which parameters are—and which are not—appropriate for their specific study.

This document is intended to be a living document, which we propose is revisited and amended annually by interested members of the community, who are encouraged to contact the authors of this document. Parts of this document were developed at the annual International Nanomedicine Conference in Sydney, Australia: <http://www.oznanomed.org/>, which will continue to act as a venue for their review and development, and interested members of the community are encouraged to attend.

After filling out the following pages, this checklist document can be attached as a “Supporting Information” document during submission of a manuscript to inform Editors and Reviewers (and eventually readers) that all points of MIRIBEL have been considered.

Supplementary Table 1. Material characterization*

Question	Yes	No
1.1 Are “ best reporting practices ” available for the nanomaterial used? For examples, see <i>Chem. Mater.</i> 28 (2016) 3535; http://doi.org/10.1021/acs.chemmater.6b01854 and <i>Chem. Mater.</i> 29 (2017) 1; http://doi.org/10.1021/acs.chemmater.6b05235		N/A
1.2 If they are available, are they used ? If not available, ignore this question and proceed to the next one.		
1.3 Are extensive and clear instructions reported detailing all steps of synthesis and the resulting composition of the nanomaterial? For examples, see <i>Chem. Mater.</i> 26 (2014) 1765; http://doi.org/10.1021/cm500632c , and <i>Chem. Mater.</i> 26 (2014) 2211; http://doi.org/10.1021/cm5010449 . Extensive use of photos, images, and videos are strongly encouraged. For example, see <i>Chem. Mater.</i> 28 (2016) 8441; http://doi.org/10.1021/acs.chemmater.6b04639	✓	
1.4 Is the size (or dimensions , if non-spherical) and shape of the nanomaterial reported?	✓	
1.5 Is the size dispersity or aggregation of the nanomaterial reported?	✓	
1.6 Is the zeta potential of the nanomaterial reported?		✓
1.7 Is the density (mass/volume) of the nanomaterial reported?	✓	
1.8 Is the amount of any drug loaded reported? ‘Drug’ here broadly refers to functional cargos (e.g., proteins, small molecules, nucleic acids).	✓	
1.9 Is the targeting performance of the nanomaterial reported, including amount of ligand bound to the nanomaterial if the material has been functionalised through addition of targeting ligands?	✓	
1.10 Is the label signal per nanomaterial/particle reported? For example, fluorescence signal per particle for fluorescently labelled nanomaterials.	✓	
1.11 If a material property not listed here is varied, has it been quantified ?	✓	
1.12 Were characterizations performed in a fluid mimicking biological conditions ?	✓	
1.13 Are details of how these parameters were measured/estimated provided?	✓	
Explanation for No (if needed):		

*Ideally, material characterization should be performed in the same biological environment as that in which the study will be conducted. For example, for cell culture studies with nanoparticles, characterization steps would ideally be performed on nanoparticles dispersed in cell culture media. If this is not possible, then characteristics of the dispersant used (e.g., pH, ionic strength) should mimic as much as possible the biological environment being studied.

Supplementary Table 2. Biological characterization*

Question	Yes	No
2.1 Are cell seeding details , including number of cells plated, confluency at start of experiment, and time between seeding and experiment reported?	✓	
2.2 If a standardised cell line is used, are the designation and source provided?	✓	
2.3 Is the passage number (total number of times a cell culture has been subcultured) known and reported?	✓	
2.4 Is the last instance of verification of cell line reported? If no verification has been performed, is the time passed and passage number since acquisition from trusted source (e.g., ATCC or ECACC) reported? For information, see <i>Science</i> 347 (2015) 938; http://doi.org/10.1126/science.347.6225.938		✓
2.5 Are the results from mycoplasma testing of cell cultures reported?		✓
2.6 Is the background signal of cells/tissue reported? (E.g., the fluorescence signal of cells without particles in the case of a flow cytometry experiment.)	✓	
2.7 Are toxicity studies provided to demonstrate that the material has the expected toxicity, and that the experimental protocol followed does not?	✓	
2.8 Are details of media preparation (type of media, serum, any added antibiotics) provided?	✓	
2.9 Is a justification of the biological model used provided? For examples for cancer models, see <i>Cancer Res.</i> 75 (2015) 4016; http://doi.org/10.1158/0008-5472.CAN-15-1558 , and <i>Mol. Ther.</i> 20 (2012) 882; http://doi.org/10.1038/mt.2012.73 , and <i>ACS Nano</i> 11 (2017) 9594; http://doi.org/10.1021/acsnano.7b04855	✓	
2.10 Is characterization of the biological fluid (<i>ex vivo/in vitro</i>) reported? For example, when investigating protein adsorption onto nanoparticles dispersed in blood serum, pertinent aspects of the blood serum should be characterised (e.g., protein concentrations and differences between donors used in study).		N/A
2.11 For animal experiments , are the ARRIVE guidelines followed? For details, see <i>PLOS Biol.</i> 8 (2010) e1000412; http://doi.org/10.1371/journal.pbio.1000412		N/A

Explanation for **No** (if needed):

*For *in vitro* experiments (e.g., cell culture), *ex vivo* experiments (e.g., in blood samples), and *in vivo* experiments (e.g., animal models). The questions above that are appropriate depend on the type of experiment conducted.

Supplementary Table 3. Experimental details*

Question	Yes	No
3.1 For cell culture experiments: are cell culture dimensions including type of well, volume of added media , reported? Are cell types (i.e.; adherent vs suspension) and orientation (if nonstandard) reported?	✓	
3.2 Is the dose of material administered reported? This is typically provided in nanomaterial mass, volume, number, or surface area added. Is sufficient information reported so that regardless of which one is provided, the other dosage metrics can be calculated (i.e. using the dimensions and density of the nanomaterial)?	✓	
3.3 For each type of imaging performed, are details of how imaging was performed provided, including details of shielding, non-uniform image processing , and any contrast agents added?	✓	
3.4 Are details of how the dose was administered provided, including method of administration, injection location, rate of administration , and details of multiple injections ?		N/A
3.5 Is the methodology used to equalise dosage provided?		N/A
3.6 Is the delivered dose to tissues and/or organs (in vivo) reported, as % injected dose per gram of tissue (%ID g ⁻¹)?		N/A
3.7 Is mass of each organ/tissue measured and mass of material reported?		N/A
3.8 Are the signals of cells/tissues with nanomaterials reported? For instance, for fluorescently labelled nanoparticles, the total number of particles per cell or the fluorescence intensity of particles + cells, at each assessed timepoint.	✓	
3.9 Are data analysis details , including code used for analysis provided?	✓	

<p>3.10 Is the raw data or distribution of values underlying the reported results provided? For examples, see <i>R. Soc. Open Sci.</i> 3 (2016) 150547; http://doi.org/10.1098/rsos.150547, https://opennessinitiative.org/making-your-data-public/, http://journals.plos.org/plosone/s/dataavailability, and https://www.nature.com/sdata/policies/repositories</p>	✓	
<p>Explanation for No (if needed):</p>		

* The use of protocol repositories (e.g., *Protocol Exchange* <http://www.nature.com/protocolexchange/>) and published standard methods and protocols (e.g., *Chem. Mater.* **29** (2017) 1; <http://doi.org/10.1021/acs.chemmater.6b05235>, and *Chem. Mater.* **29** (2017) 475; <http://doi.org/10.1021/acs.chemmater.6b05481>) are encouraged.

References

- 1 J. Edward Semple, B. Sullivan, T. Vojtkovsky and K. N. Sill, *J. Polym. Sci. Part A Polym. Chem.*, 2016, 54, 2888–2895.
- 2 M.H. Randall, P.R. Buzby, T.J. Erickson, J.D. Trometer, J.J. Miller Jr, D.G. Ahern, and M.N. Bobrow, *NEN Life Science Products Inc*, 2000. Cyanine dyes and synthesis methods thereof. U.S. Patent 6,114,350.
- 3 Y. Kim, M. H. Pourgholami, D. L. Morris, H. Lu and M. H. Stenzel, *Biomater. Sci.*, 2013, 1, 265–275.
- 4 A. K. Pearce, J. D. Simpson, N. L. Fletcher, Z. H. Houston, A. V. Fuchs, P. J. Russell, A. K. Whittaker and K. J. Thurecht, *Biomaterials*, 2017, 141, 330–339.
- 5 B. Howard, N. Fletcher, Z. H. Houston, A. V. Fuchs, N. R. B. Boase, J. D. Simpson, L. J. Raftery, T. Ruder, M. L. Jones, C. J. de Bakker, S. M. Mahler and K. J. Thurecht, *Adv. Healthc. Mater.*, 2016, 5, 2055–2068.
- 6 Y. Zhao, N. L. Fletcher, A. Gemmell, Z. H. Houston, C. B. Howard, I. Blakey, T. Liu and K. J. Thurecht, *Adv. Ther.*, 2020, 3, 1900202.